

A Successive-Elimination Approach to Adaptive Robotic Sensing

Esther Rolf* David Fridovich-Keil† Max Simchowitz‡ Benjamin Recht§
 Claire Tomlin¶

November 12, 2021

Abstract

We study the adaptive sensing problem for the multiple source seeking problem, where a mobile robot must identify the strongest emitters in an environment with background emissions. Background signals may be highly heterogeneous, and can mislead algorithms which are based on receding horizon control, greedy heuristics, or smooth background priors. We propose **AdaSearch**, a general algorithm for adaptive sensing. **AdaSearch** combines global trajectory planning with principled confidence intervals in order to concentrate measurements in promising regions while still guaranteeing sufficient coverage of the entire area. Theoretical analysis shows that **AdaSearch** significantly outperforms a uniform sampling strategy when the distribution of background signals is highly variable. Simulation studies demonstrate that when applied to the problem of radioactive source-seeking, **AdaSearch** outperforms both uniform sampling and a receding time horizon information-maximization approach based on the current literature. We corroborate these findings with a hardware demonstration, using a small quadrotor helicopter in a motion-capture arena.

1 Introduction

We introduce a new approach to the adaptive sensing problem, in which a robot must traverse an environment to identify locations or items of interest. Adaptive sensing encompasses many well-studied problems in robotics, including the rapid identification of accidental contamination leaks and radioactive sources [1, 2], and finding individuals in search and rescue missions [3]. In such settings, it is often critical to devise a sensing trajectory that returns a correct solution as quickly as possible. We focus on the problem of radiocative source-seeking (RSS), in which a UAV (Fig. 1) must identify the k -largest radioactive emitters in its environment, where k is a user-defined parameter. RSS is a particularly interesting instance of the adaptive sensing problem, due both to the challenges posed by the highly heterogeneous background noise [4], as well as to the existence of a well-characterized sensor model amenable to the construction of statistical confidence intervals. We emphasize, however, that our main contribution, **AdaSearch**, generalizes to other settings with multiple signal sources and a heterogeneous background.

The current state of the art for this type of problem is information maximization, in which measurements are collected in the most promising locations, following a receding planning horizon. Information maximization is appealing because it favors measuring regions that are likely to contain the highest emitters, and avoids wasting time elsewhere. However, when operating in real-time, computational constraints necessitate approximations such as limits on planning horizon and trajectory parameterization. These limitations scale with size of the search region and complexity of the sensor model, and they may cause the algorithm to be excessively greedy and spend too much time tracking down false leads.

We introduce **AdaSearch**, a successive-elimination framework for general adaptive sensing problems, and demonstrate it within the context of RSS. **AdaSearch** explicitly maintains confidence intervals over the

*UC Berkeley, CA. erolf@berkeley.edu

†UC Berkeley, CA. dfk@berkeley.edu

‡UC Berkeley, CA. msimchow@berkeley.edu

§UC Berkeley, CA. brecht@berkeley.edu

¶UC Berkeley, CA. tomlin@eecs.berkeley.edu

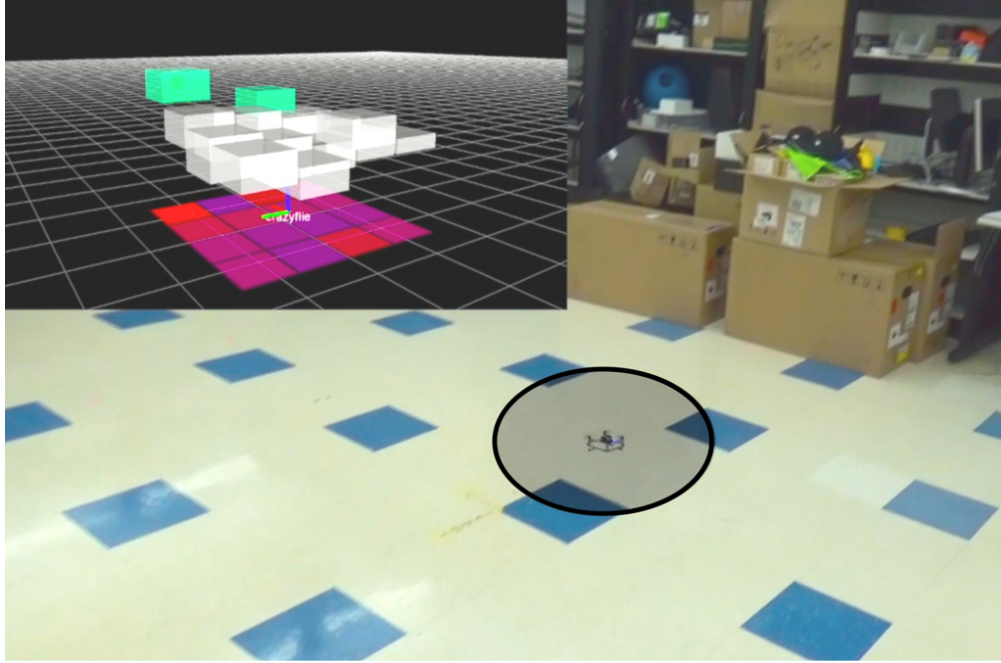


Figure 1: A Crazyflie 2.0 quadrotor in a motion capture arena. Inset shows radiactivity estimates and confidence intervals.

emissions rate at each point in the environment. Using these confidence intervals, the algorithm identifies a set of candidate points likely to be among the top emitters, and eliminates points which are not.

Rather than iteratively planning for short, receding time horizons, `AdaSearch` repeats a *fixed, globally-planned path*, adjusting the robot’s speed in real-time to focus measurements on promising regions. This approach offers coverage of the full search space while affording an adaptive measurement allocation in the spirit of information maximization. By maintaining a single fixed, global path, we reduce the online computational overhead, yielding an algorithm easily amenable to real-time implementation.

In simulations (Sec. 6), we find that `AdaSearch` significantly outperforms an implementation of information maximization based on [5]. While initially surprising, this suggests that either our confidence interval approach yields a more efficient measurement allocation, or that the receding horizon in information maximization causes it to be misled by spurious background signals. To disambiguate between these two effects, we compare `AdaSearch` to a uniform search algorithm which follows the same global path as `AdaSearch` but at a uniform speed. Simulations and theoretical results demonstrate that `AdaSearch` excels in situations where background signals are heterogeneous. Surprisingly, this uniform procedure with global planning also outperforms the information maximization method, but by a smaller margin than `AdaSearch`. This suggests that the global path is an important factor in `AdaSearch`’s success. Finally, we corroborate these findings with a hardware demonstration, using a quadrotor helicopter in a motion capture arena.

2 Related Work

Adaptive, or active, robotic sensing is central to problems in environmental monitoring [6, 1, 2], and encompasses many different modeling choices and algorithmic methods.

Information maximization methods. One of the most popular approaches to robotic source-seeking, notably in active localization [7] and target localization [8], is to choose trajectories that maximize some measure of information [9, 10, 11, 7]. Planning for information maximization-based methods typically proceeds with a receding horizon [9, 12, 5, 13, 14]. In the specific case of linear Gaussian measurements, Atanasov et al. [15] formulate the informative path planning problem as an optimal control problem which affords an offline solution.

Marchant et. al. [12] combine upper confidence bounds (UCBs) at potential source locations with

a penalization term for travel distance to define a greedy acquisition function for Bayesian optimization. Their follow up work [5] reasons at the path level to find longer, more informative trajectories. Noting the limitations of a greedy receding horizon approach, [16] incentivizes exploration by using a look-ahead step in planning. Recently, [10] encodes a notion of spatial hierarchy in designing informative trajectories, based on a multi-armed bandit formulation. While [10] and AdaSearch are similarly motivated, hierarchical planning is inefficient for many sensing models, e.g. for short-range sensors, or signals that decay quickly with distance from the source.

Gaussian processes for information maximization. Information maximization methods require a prior distribution on the underlying signals. Many works in active sensing model this prior as being drawn from a Gaussian process (GP) over an underlying space of possible functions [8, 9, 12]. The GP prior tacitly enforces the assumption that the sensed signal is smooth [12]. In certain applications, this is well motivated by physical laws, e.g. diffusion [16]. However, GP priors may not reflect the sparse, heterogeneous emissions encountered in radiation detection and similar problem settings.

Multi-armed bandit approaches. AdaSearch draws heavily on confidence-bound based algorithms from the pure exploration bandit literature [17, 18, 19]. In contrast to these works, our method allows for efficient measurement allocation despite the spatial constraints of movement inherent to mobile robotic sensing, and explicitly incorporates a realistic sensor model. Other works have studied spatial constraints in the online, “adversarial” reward setting [20, 21]. One can also study bandit algorithms from a Bayesian perspective, where a prior is placed over underlying rewards. For example, [22] provides an interpretation of GP-UCB in terms of information maximization. AdaSearch is similar to the lower and upper confidence bound (LUCB) algorithm [23], but opts for successive elimination over the more aggressive LUCB sampling strategy to afford efficient traversal of the search space.

Other source-seeking methods. Modeling emissions as a continuous field, gradient-based approaches estimate and follow the gradient of the measured signal toward local maxima [24, 25, 26]. One of the key drawbacks of gradient-based methods is their susceptibility to finding local, rather than global, extrema. Moreover, the error margin on the noise of gradient estimators for large-gain sensors measuring noisy signals can be prohibitively large [27], as is the case in RSS.

3 AdaSearch Planning Strategy

Problem Statement. We consider signals (e.g. radiation) which emanate from a finite set of environment points \mathcal{S} . Each point $x \in \mathcal{S}$ emits signals $\{\mathbf{X}_t(x)\}$ indexed by time t with means $\mu(x)$, independent and identically distributed over time. Our aim is to correctly and exactly discern the set of the k points in the environment which emit the maximal signals:

$$\mathcal{S}^*(k) = \arg \max_{\substack{S' \subseteq \mathcal{S} \\ |S'|=k}} \sum_{x \in S'} \mu(x) \quad (1)$$

for a prespecified integer $1 \leq k \leq |\mathcal{S}|$. Throughout, we assume that $\mathcal{S}^*(k)$ is unique.

In order to decide which points are maximal emitters, the robot takes sensor measurements along a fixed path $\mathcal{Z} = (z_1, \dots, z_n)$ in the robot’s configuration space. Measurements are determined by a known *sensitivity function* $h(x, z)$ that describes the contribution of environment point $x \in \mathcal{S}$ to a sensor measurement collected from sensing configuration $z \in \mathcal{Z}$. We consider a linear sensing model in which the total observed measurement at time t , $\mathbf{Y}_t(z)$, taken from sensing configuration z , is the weighted sum of the contributions $\{\mathbf{X}_t(x)\}$ from all environment points:

$$\mathbf{Y}_t(z) = \sum_{x \in \mathcal{S}} h(x, z) \mathbf{X}_t(x) \quad (2)$$

Note that while $h(x, z)$ is known, the $\{\mathbf{X}_t\}$ are unknown, and must be estimated via the observations $\{\mathbf{Y}_t\}$.

The path of sensing configurations, \mathcal{Z} , should be as short as possible, yet also provide sufficient information about the entire environment. This may be expressed as a condition on the minimum aggregate sensitivity α to any given environment point x over the sensing path \mathcal{Z} :

$$\sum_{z \in \mathcal{Z}} h(x, z) \geq \alpha > 0 \quad \forall x \in \mathcal{S} \quad (3)$$

Algorithm 1: AdaSearch

- 1 **Input** Candidate points of interest \mathcal{S} ; Sensing path of configurations \mathcal{Z} ; Number of points of interest k ; Minimum measurement duration τ_0 ; Procedure for constructing $[\text{LCB}_i(x), \text{UCB}_i(x)]$ (e.g., as in Sections 4.1 and 4.2); confidence parameter δ_{tot} .
- 2 **Initialize** $\mathcal{S}_0^{\text{top}} = \emptyset, \mathcal{S}_0 = \mathcal{S}$
- 3 **For** rounds $i = 0, 1, 2, \dots$
- 4 **If** $\mathcal{S}_i = \emptyset$, **Return** $\mathcal{S}_i^{\text{top}}$
- 5 **Choose** configuration subset $\mathcal{Z}_i \subseteq \mathcal{Z}$ which is informative about environment points $x \in \mathcal{S}_i$.
- 6 **Execute** a trajectory along path \mathcal{Z} which spends time $\tau_i = \tau_0 \cdot 2^i$ at each $z \in \mathcal{Z}_i$, and time τ_0 at each $z \in \mathcal{Z} \setminus \mathcal{Z}_i$. Meanwhile, observe signal measurements according to (2).
- 7 **Update** $[\text{LCB}_i(x), \text{UCB}_i(x)]$ for all $x \in \mathcal{S}$.
- 8 **Update** Augment $\mathcal{S}_i^{\text{top}}$ according to (4), and prune \mathcal{S}_i according to (5).

Moreover, we must be able to disambiguate between contributions from different environment points $x, x' \in \mathcal{S}$. Consider the sensitivity matrix $H \in \mathbb{R}^{|\mathcal{S}| \times |\mathcal{Z}|}$ that encodes the sensitivity of each sensing configuration $z_j \in \mathcal{Z}$ to each point $x_i \in \mathcal{S}$, so that $H_{ij} := h(x_i, z_j)$. The disambiguation constraint then translates to a rank constraint: $\text{rank}(H) \geq |\mathcal{S}|$. Sections 4.1 and 4.2 define two different sensitivity functions which we will study in the context of the RSS problem. In Section 7, we discuss sensitivity functions that may arise in other application domains.

The AdaSearch algorithm. AdaSearch (Alg. 1) proceeds by concentrating measurements in regions of uncertainty, until it is confident which points belong to $S^*(k)$. At each round i , we maintain a set of environment points $\mathcal{S}_i^{\text{top}}$ which we are confident are among the top- k , and a set of candidate points \mathcal{S}_i about which we are still uncertain. As the robot traverses the environment, new sensor measurements allow us update the confidence intervals

$$[\text{LCB}_i(x), \text{UCB}_i(x)] \text{ for each } x \in \mathcal{S}_i.$$

and prune the uncertainty set \mathcal{S}_i . The procedure for constructing these intervals from observations should ensure that for every $x \in \mathcal{S}_i$, $\text{LCB}_i(x) \leq \mu(x) \leq \text{UCB}_i(x)$ with high probability. Sections 4.1 and 4.2 detail the definition of these confidence intervals under different sensing models.

Using the updated confidence intervals, we can expand the set $\mathcal{S}_{i+1}^{\text{top}}$ and prune the set \mathcal{S}_{i+1} . The new top-set $\mathcal{S}_{i+1}^{\text{top}}$ is comprised of the old top-set $\mathcal{S}_i^{\text{top}}$ as well as all points $x \in \mathcal{S}_i$ whose lower confidence bounds exceed the upper confidence bounds of all but $(k - |\mathcal{S}_i^{\text{top}}|)$ points in \mathcal{S}_i ; formally,

$$\mathcal{S}_{i+1}^{\text{top}} \leftarrow \mathcal{S}_i^{\text{top}} \cup \{x \in \mathcal{S}_i \mid \text{LCB}_i(x) > (k - |\mathcal{S}_i^{\text{top}}| + 1)\text{-th largest } \text{UCB}_i(x'), x' \in \mathcal{S}_i\}. \quad (4)$$

Next, the points added to $\mathcal{S}_{i+1}^{\text{top}}$ are removed from \mathcal{S}_{i+1} , since we are now certain about them. Additionally, we remove all points in \mathcal{S}_i whose upper confidence bound is lower than the lower confidence bounds of at least $k - |\mathcal{S}_{i+1}^{\text{top}}|$ points in \mathcal{S}_i . The set \mathcal{S}_{i+1} is defined constructively as:

$$\mathcal{S}_{i+1} \leftarrow \{x \in \mathcal{S}_i \mid x \notin \mathcal{S}_{i+1}^{\text{top}} \text{ and } \text{UCB}_i(x) \geq (k - |\mathcal{S}_{i+1}^{\text{top}}|)\text{-th largest } \text{LCB}_i(x'), x' \in \mathcal{S}_i\}. \quad (5)$$

Trajectory planning for AdaSearch: Observe that the update rules (4) and (5) only depend on confidence intervals for points $x \in \mathcal{S}_i$. Rather than wasting time measuring points $x \notin \mathcal{S}_i$, at each round, AdaSearch chooses a subset of the sensing configurations $\mathcal{Z}_i \subseteq \mathcal{Z}$ which are informative to \mathcal{S}_i . For omnidirectional sensors, choosing \mathcal{Z}_i is relatively straightforward (see Sec. 4.3). We discuss generalizing to more sophisticated sensors in Sec. 7.

AdaSearch defines a trajectory through the informative configurations \mathcal{Z}_i by following the fixed path \mathcal{Z} over all sensing configurations, spending a minimal time τ_0 at each uninformative configuration in $\mathcal{Z} \setminus \mathcal{Z}_i$, and slowing down to spend time $2^i \tau_0$ at each informative configuration in \mathcal{Z}_i . Doubling the time spent at each $z \in \mathcal{Z}_i$ in each round amortizes the time spent traversing the entire path \mathcal{Z} . Changing only the speed, rather than the entire path, makes AdaSearch amenable to real-time operation. For omnidirectional sensors, a simple raster pattern (Fig. 2a) suffices for \mathcal{Z} ; other cases are discussed in Sec. 7.

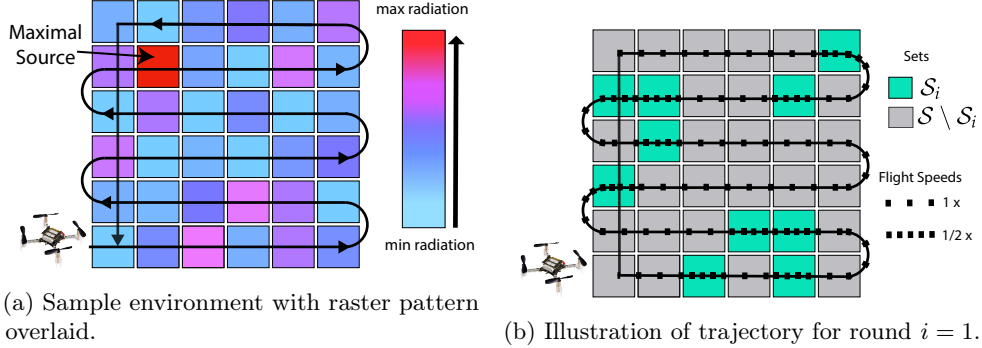


Figure 2: (a) Raster path \mathcal{Z} over an example grid environment of size 6×6 . The path ensures that each grid point is sufficiently measured during each round. (b) Illustrative trajectory for round $i = 1$. Dots indicate measurements. **AdaSearch** slows down to take twice as many measurements over points $x \in \mathcal{S}_i$.

In Appendix A, we establish the following lemma, which states that the two update rules above guarantee the overall correctness of **AdaSearch**, whenever the confidence intervals $[\text{LCB}_j(x), \text{UCB}_j(x)]$ actually contain the correct mean $\mu(x)$:

Lemma 1 (Sufficient Condition for Correctness) *For each round $i \geq 0$, $\mathcal{S}_i^{\text{top}} \cap \mathcal{S}_i = \emptyset$. Moreover, whenever the confidence intervals satisfy the coverage property:*

$$\text{for all rounds } j \leq i \text{ and all } x \in \mathcal{S}_j, \quad \mu(x) \in [\text{LCB}_j(x), \text{UCB}_j(x)], \quad (6)$$

then $\mathcal{S}_{i+1}^{\text{top}} \subseteq \mathcal{S}^(k) \subseteq \mathcal{S}_{i+1}^{\text{top}} \cup \mathcal{S}_{i+1}$. If (6) holds for all rounds i , then **AdaSearch** terminates and correctly returns $\mathcal{S}^*(k)$.*

Lemma 1 provides a backbone upon which we construct a probabilistic correctness guarantee in Sec. 5. If the event (6) holds with some probability $1 - \delta_{\text{tot}}$ over all rounds, then **AdaSearch** returns the correct set $\mathcal{S}^*(k)$ with the same probability $1 - \delta_{\text{tot}}$.

4 Radioactive Source-Seeking with Poisson Emissions

While **AdaSearch** may be used to solve a range of adaptive sensing problems, here we refine our focus to the application of **AdaSearch** to the radioactive source-seeking (RSS) problem with an omnidirectional sensor onboard a quadrotor helicopter. The environment is defined by potential emitter locations which lie on the ground plane, $x \in \mathcal{S} \subset \mathbb{R}^2 \times \{0\}$, and sensing configurations encode spatial position, $z \in \mathcal{Z} \subset \mathbb{R}^3$. Environment points emit gamma rays according to a Poisson process, i.e. $\mathbf{X}_t(x) \sim \text{Poisson}(\mu(x))$. Here, $\mu(x)$ corresponds to rate or intensity of emissions from point x .

Thus, the number of gamma rays observed over a time interval of length τ from configuration z has distribution

$$\mathbf{Y}_t(z) \sim \text{Poisson}(\tau \cdot \sum_{x \in \mathcal{S}} h(x, z) \mu(x)), \quad (7)$$

where $h(x, z)$ is specified by the sensing model. In the following sections, we introduce two sensing models: a pointwise sensing model amenable to theoretical analysis (Sec. 4.1), and a more physically realistic sensing model for the RSS problem (Sec. 4.2).

In both settings, we develop appropriate confidence intervals for use in the **AdaSearch** algorithm. We introduce the specific path used for global trajectory planning in Sec. 4.3. Finally, we conclude with two benchmark algorithms to which we compare **AdaSearch** (Sec. 4.4) for the RSS problem.

4.1 Pointwise Sensing Model

First, we consider a simplified sensing model, where the set of sensing locations \mathcal{Z} coincides with the set \mathcal{S} of all emitters, i.e. each $z \in \mathcal{Z}$ corresponds to precisely one $x \in \mathcal{S}$ and vice versa. The sensitivity function is

defined as

$$h(x, z) = \mathbb{I}(x = z) = \begin{cases} 1 : x = z \\ 0 : x \neq z \end{cases} .$$

Now we derive confidence intervals for Poisson counts observed according to this sensing model. Define $\mathbf{N}(x)$ to be the total number of gamma rays observed during the time interval of length τ spent at x . The maximum likelihood estimator (MLE) of the emission rate for point x is $\hat{\mu}(x) = \frac{\mathbf{N}(x)}{\tau}$. In Appendix B, we introduce the *bounding functions* $U_-(\cdot, \cdot)$ and $U_+(\cdot, \cdot)$, and show that for any $\lambda \geq 0$, $\mathbf{N} \sim \text{Poisson}(\lambda)$, and $\tilde{\delta} \in (0, 1)$,

$$\Pr[U_-(\mathbf{N}, \tilde{\delta}) \leq \lambda \leq U_+(\mathbf{N}, \tilde{\delta})] \geq 1 - 2\tilde{\delta}.$$

Let $\mathbf{N}_i(x)$ denote the number of gammas rays observed from emitter x during round i , so that $\mathbf{N}(x) \sim \text{Poisson}(\tau_i \mu(x))$. For any point $x \in \mathcal{S}_i$, the corresponding duration of measurement would be τ_i . The bounding functions above provide the desired confidence intervals for signals $\mu(x), \forall x \in \mathcal{S}_i$:

$$\text{LCB}_i(x) := \frac{1}{\tau_i} U_-(\mathbf{N}_i(x), \delta_i) , \quad \text{UCB}_i(x) := \frac{1}{\tau_i} U_+(\mathbf{N}_i(x), \delta_i) , \quad (8)$$

This bound implies that the inequality $\tau_i \text{LCB}_i(x) \leq \tau_i \mu(x) \leq \tau_i \text{UCB}_i(x)$ holds with probability $1 - 2\delta_i$. Dividing by τ_i , we see that $\text{LCB}_i(x)$ and $\text{UCB}_i(x)$ are valid confidence bounds for $\mu(x)$.

The term δ_i can be thought of as an “effective confidence” for each interval that we construct during round i . In order to achieve the correctness in Lemma 1 with overall probability $1 - \delta_{\text{tot}}$, we set the effective confidence δ_i at each round to be $\delta_i = \delta_{\text{tot}}/(8|\mathcal{S}|i^2)$ (see Appendix C.3). As the number of confidence intervals we reason about increases, we must be more confident about each individual interval in order to retain a total confidence of $1 - \delta_{\text{tot}}$. Thus, δ_i is decreasing in both the round number i and the environment size $|\mathcal{S}|$.

4.2 Physical Sensing Model

A more physically accurate sensing model for RSS reflects that, in general, the gamma ray count at each location is a sensitivity-weighted combination of the emissions from each environment point. Conservation of energy allows us to approximate the sensitivity function with an inverse-square law $h(x, z) := c/\|x - z\|_2^2$, where c is a known, sensor-dependent constant.

Because multiple environment points x contribute to the counts observed from any sensor position z , the MLE $\hat{\mu}$ for the emission rates at all $x \in \mathcal{S}$ is difficult to compute efficiently. However, we can approximate it in the limit: $\frac{1}{\sqrt{\tau}} \text{Poisson}(\tau\mu) \xrightarrow{d} \mathcal{N}(\mu, \mu)$ as $\tau \rightarrow \infty$. Thus, we may compute $\hat{\mu}$ as the least squares solution:

$$\hat{\mu} = \arg \min_{\vec{\mu}} \|\tilde{H}^T \vec{\mu} - \vec{\mathbf{Y}}\|_2^2 , \quad (9)$$

where $\vec{\mu} \in \mathbb{R}^{|\mathcal{S}|}$ is a vector representing the mean emissions from each $x \in \mathcal{S}$, $\vec{\mathbf{Y}} \in \mathbb{R}^m$ is a vector representing the observed number of counts at each of m consecutive time intervals, and $\tilde{H} \in \mathbb{R}^{|\mathcal{S}| \times m}$ is a rescaled sensitivity matrix such that \tilde{H}_{ij} gives the measurement-adjusted sensitivity of the i^{th} environment point to the sensor at the j^{th} sensing position.¹ The resulting confidence bounds are given by the standard Gaussian confidence bounds:

$$[\text{LCB}_i(x_k), \text{UCB}_i(x_k)] := \hat{\mu}(x_k) \pm \alpha(\delta_i) \cdot \Sigma_{kk}^{1/2} \quad \text{where } \Sigma := (\tilde{H} \tilde{H}^T)^{-1} \quad (10)$$

where $\alpha(\delta_i)$ controls the round-wise effective confidence widths in equation (10) as a function of the desired maximum probability of overall error, δ_{tot} . We use a Kalman filter to solve the least squares problem (9) and compute the confidence intervals (10).

¹Explicitly stated, $\tilde{H}_{ij} = h(x_i, z_j)/(\mathbf{Y}_j + b)$, The rescaling term $\mathbf{Y}_j + b$ is a plug-in estimator for the variance of measurement \mathbf{Y}_j (with small bias b introduced for numerical stability), which serves to downweight measurements with higher variance.

4.3 Design and Planning for AdaSearch.

Pointwise sensing model. In the pointwise sensing model, $\mathcal{Z} = \mathcal{S}$ and the informative measurements about the signal value $\mu(x)$ can only be obtained from location $z = x$. Hence, the informative sensing locations \mathcal{Z}_i at round i are precisely \mathcal{S}_i . We therefore choose the path \mathcal{Z} to be a simple space filling curve over a raster grid, depicted in Fig. 2a, which provides coverage of all of \mathcal{S} . We adopt a simple dynamical model of the quadrotor in which it can fly at up to a pre-specified top speed, and where acceleration and deceleration times are negligible. This model is reasonably accurate for large outdoor environments where travel times are dominated by movement at maximum speed. We let τ_0 denote the time required for the quadrotor to traverse a given grid pixel $x \in \mathcal{S}$ at top speed. Figure 2a shows an example environment with a raster pattern trajectory overlaid, while Fig. 2b illustrates the trajectory followed during round $i = 1$ (recall that i begins at 0) with desired measurement locations \mathcal{Z}_i shown in green.

Physical sensing model. Because the physical sensitivity follows an inverse-square law, the most informative measurements about $\mu(x)$ are those taken at locations z near to x . Hence, we restrict measurement locations to the points $z \in \mathbb{R}^3$ one meter vertically offset above points $x \in \mathcal{S}$ on the ground plane. We use the same design and planning strategy as in the point-wise measurement model, following the raster pattern depicted in Fig. 2a.

4.4 Baselines

To demonstrate the effectiveness of AdaSearch, we compare it to two baselines: a uniform-sampling based algorithm `NaiveSearch`, and a spatially-greedy information maximization algorithm `InfoMax`.

NaiveSearch algorithm. As a non-adaptive baseline, we consider a uniform sampling scheme that follows the raster pattern in Fig. 2a at constant speed. This global `NaiveSearch` trajectory results in measurements uniformly spread over the grid, and avoids redundant movements between sensing locations. The only difference between `NaiveSearch` and AdaSearch is that `NaiveSearch` flies at a constant speed, while AdaSearch varies its speed adaptively in response to measurements it has collected so far. For $k = 1$ emitter, `NaiveSearch` terminates at the first round i in which $\text{LCB}_i(x) > \text{UCB}_i(x'), \forall x' \in \mathcal{S} \setminus \{x\}$ for some environment point x . The general termination criterion for $k \geq 1$ is described in Appendix B. Comparing to `NaiveSearch` serves to measure the advantages of AdaSearch’s adaptive measurement allocation separately from the effects of its global trajectory heuristic.

InfoMax algorithm. As discussed in Sec. 2, one of the most successful methods for active search in robotics is receding horizon informative path planning, e.g. [5, 13]. We implement `InfoMax`, a version of this approach based on [5] and specifically adapted for RSS. Each planning invocation solves an information maximization problem over the space of trajectories $\xi : [t, t + T_{\text{plan}}] \rightarrow \mathcal{B}$ mapping from time in the next T_{plan} seconds to a box $\mathcal{B} \subset \mathbb{R}^3$.

We measure the information content of a candidate trajectory ξ by accumulating the sensitivity-weighted variance at each grid point $x \in \mathcal{S}$ at N evenly-spaced times along ξ , i.e.

$$\xi_t^* = \arg \max_{\xi} \sum_{i=1}^N \sum_{j=1}^{|\mathcal{S}|} \Sigma_{jj} \cdot h(x_j, \xi(t + T_{\text{plan}}i/N)) . \quad (11)$$

This objective favors taking measurements sensitive to regions with high uncertainty. As a consequence of the Poisson emissions model, these regions will also generally have high expected intensity μ ; therefore we expect this algorithm to perform well for the RSS task. We parameterize trajectories ξ as Bezier curves in \mathbb{R}^3 , and use Bayesian optimization (see [28]) to solve (11) because of the high computational cost of evaluating the objective function. Empirically, we found that Bayesian optimization outperformed both naive random search and a finite difference gradient method. We set T_{plan} to 10 s and used second-order Bezier curves. Longer time horizons and higher order Bezier curves quickly become intractable in real time.

Stopping criteria and metrics. All three algorithms use the same stopping criterion, which is satisfied when the k^{th} highest LCB exceeds the $(k+1)^{\text{th}}$ highest UCB. For sufficiently small probability of error δ_{tot} , this ensures that the top- k sources are almost always correctly identified by all algorithms; they are always correctly identified in all experiments in Sec. 6.

5 Theoretical Runtime Analysis

We now present a theoretical runtime analysis for **AdaSearch** and **NaiveSearch**, under the pointwise sensing model from Sec. 4.1. For simplicity, we will present our the result for $k = 1$. Proofs, along with general results for arbitrary k , and complimentary lower bounds, are presented in Appendix B.

Our analysis shows that both algorithms correctly identify the maximal source with high probability, and sharply quantifies the relative advantage of **AdaSearch** over **NaiveSearch** in terms of the distribution of the background radiation. The empirical results presented in Sec. 6 validate the correctness of both algorithms, and show that our theoretical results are predictive of the relative performance of **AdaSearch** and **NaiveSearch** in simulation.

We analyze **AdaSearch** with the trajectory planning strategy outlined in Sec. 4.3. For **NaiveSearch**, the robot spends time τ_i at each point in each round i until termination, which is determined by the same confidence intervals and termination criterion for **AdaSearch**.

We will be concerned with the *total runtime*, defined as

$$T^{\text{run}} = \begin{cases} \sum_{i=0}^{i_{\text{fin}}} (\tau_i |\mathcal{S}_i| + \tau_0 |\mathcal{S} \setminus \mathcal{S}_i|) & (\text{AdaSearch}) \\ \sum_{i=0}^{i_{\text{fin}}} \tau_i |\mathcal{S}| & (\text{NaiveSearch}) \end{cases},$$

where i_{fin} denotes the round at which the algorithm terminates. Since $k = 1$, we shall replace $\mathcal{S}^*(k)$ with x^* . Our bounds will be stated in terms of the divergences

$$d(\mu(x), \mu^*) := \frac{(\mu^* - \mu(x))^2}{\mu^*},$$

which approximate the KL-divergence between the distribution $\text{Poisson}(\mu^*)$ and $\text{Poisson}(\mu_k)$ (Lemma 4 in Appendix B), and therefore the sample complexity of distinguishing between the maximal source and a source emitting photons at rate $\mu(x)$. Our main theorem is as follows:

Proposition 2 Define the adaptive and uniform sample complexity terms $\mathcal{C}_{\text{adapt}}$ and $\mathcal{C}_{\text{unif}}$:

$$\mathcal{C}_{\text{adapt}} := \sum_{x \in \mathcal{S} \setminus \{x^*\}} \left(\tau_0 + \frac{1}{d(\mu(x), \mu^*)} \right) \quad \text{and} \quad \mathcal{C}_{\text{unif}} := |\mathcal{S}| \left(\tau_0 + \max_{x \in \mathcal{S}} \frac{1}{d(\mu(x), \mu^*)} \right). \quad (12)$$

No matter the distribution of emitters in the environment, $\mathcal{C}_{\text{adapt}} \leq \mathcal{C}_{\text{unif}}$. Then for any $\delta_{\text{tot}} > 0$, **NaiveSearch** executed with confidence parameter δ_{tot} returns the correct maximal source x^* and satisfies the following guarantee with probability $1 - \delta_{\text{tot}}$:

$$T^{\text{run}}(\text{NaiveSearch}) \leq \mathcal{C}_{\text{unif}} \cdot \tilde{\mathcal{O}}(\log(|\mathcal{S}|/\delta_{\text{tot}})).$$

Moreover, with probability $1 - \delta_{\text{tot}}$, **AdaSearch** returns the correct maximal source x^* and satisfies the guarantee:

$$T^{\text{run}}(\text{AdaSearch}) \leq \mathcal{C}_{\text{adapt}} \cdot \tilde{\mathcal{O}}(\log(|\mathcal{S}|/\delta_{\text{tot}})) + \mathcal{O}(|\mathcal{S}| \log(\mathcal{C}_{\text{unif}}/|\mathcal{S}|)).$$

The $\tilde{\mathcal{O}}(\log(|\mathcal{S}|/\delta_{\text{tot}}))$ accounts for travel times of transitioning between measurement configurations. The second term $|\mathcal{S}| \log(\mathcal{C}_{\text{unif}}/|\mathcal{S}|)$ accounts for the travel time of traversing the uninformative points in the global path \mathcal{Z} at a high speed. Observe that this term is never larger than the term $T^{\text{run}}(\text{NaiveSearch})$, and is typically dominated by $\mathcal{C}_{\text{adapt}} \cdot \tilde{\mathcal{O}}(\log(|\mathcal{S}|/\delta_{\text{tot}}))$. With a uniform strategy, the number of measurements (and hence the total time) scales with the *largest value* of $1/d(\mu(x), \mu^*)$ over $x \in \mathcal{S}$ because that quantity alone determines the number of rounds required. In contrast, **AdaSearch** scales with the *average* of $1/d(\mu(x), \mu^*)$ because it dynamically chooses which regions to sample more precisely. In experiments, we validate that when the values of $d(\mu(x), \mu^*)$ are heterogeneous, **AdaSearch** yields significant speedups over **NaiveSearch**.

Runtime Comparison

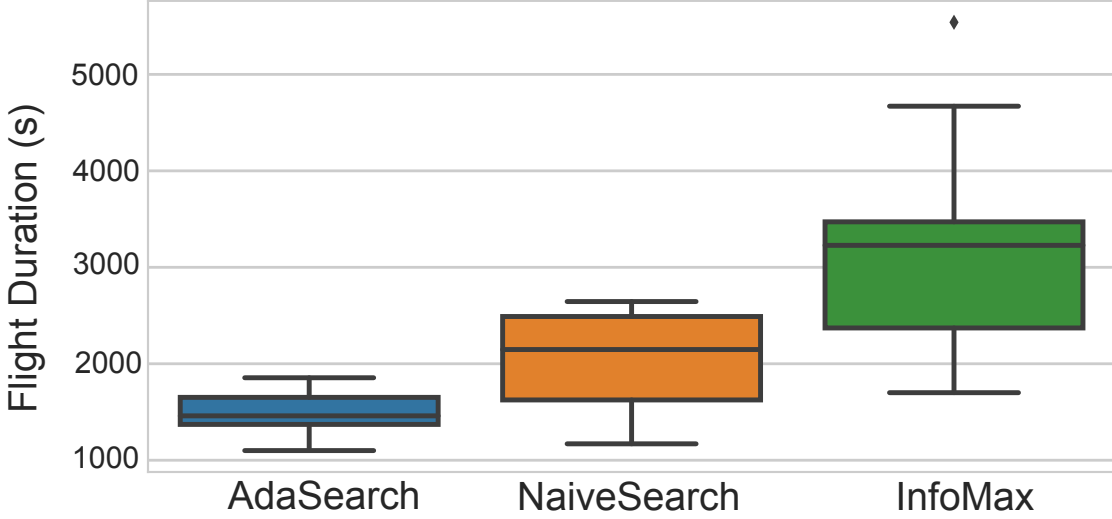


Figure 3: Runtimes of `AdaSearch`, `NaiveSearch`, and `InfoMax` over 10 randomized trials with $\bar{\mu} = 400$ and $\mu^* = 800 \frac{\text{counts}}{\text{s}}$.

6 Experiments

We compare the performance of `AdaSearch` with the baselines defined in Sec. 4.4 in simulation for the RSS problem, and validate `AdaSearch` in a hardware demonstration.

Simulation methodology. We evaluate `AdaSearch`, `InfoMax`, and `NaiveSearch` in simulation using the Robot Operating System (ROS) framework [29]. The environment points \mathcal{S} lie in a 16×16 planar grid, spread evenly over a total area $64 \times 64 \text{ m}^2$. Radioactive emissions are detected by a simulated sensor following the physical sensing model in Sec 4.2. We set $k = 1$, so that the set $\mathcal{S}^*(k) = \{x^*\}$ is a single point in the environment. We then fix a maximum emission rate $\mu^* = \mu(x^*) = 800$ photons/s, as well as a parameter $\bar{\mu} \in \{300, 400, 500, 600\}$ photons/s governing the maximum rate of emissions for background radiation.

For each setting of $\bar{\mu}$, we test all three algorithms on 10 grids randomly generated as follows. For each point $x \in \mathcal{S}$, we draw the mean emissions $\mu(x)$ uniformly at random in the interval $[0, \bar{\mu}]$. Then, we choose one point uniformly at random from the grid as the maximal point source x^* , which we set to emit at rate $\mu(x^*) = \mu^*$. All mean intensities remain fixed throughout the trial, but are randomized between trials. Finally, we execute all three algorithms on each of the 10 instantiated grids in a real-time simulation, using approximate near-hover quadrotor dynamics controlled by a stabilizing linear feedback controller.

Results. We analyze performance with respect to the following metrics: (a) total runtime (time from takeoff until x^* is located with confidence), (b) absolute difference between the predicted and actual emission rate of the maximal source x^* , and (c) deviation of the estimated source emissions from the ground truth emission rates over the entire environment, measured in the Euclidean norm. Fig. 3 plots the runtimes for each algorithm for $\bar{\mu} = 400$. The uniform baseline `NaiveSearch` terminates significantly earlier than `InfoMax`, and `AdaSearch` terminates even earlier, on average. The comparison between `NaiveSearch` and `InfoMax` may seem surprising, because one would expect `InfoMax` to seek out higher-variance points (which are also higher mean), and thereby outperform uniform sampling.

Fig. 4a plots the absolute difference in the estimated emission rate $\hat{\mu}$ and the true emission rate μ at x^* . `AdaSearch` and `NaiveSearch` perform comparably over time, though `AdaSearch` terminates significantly earlier. Fig. 4b plots the total Euclidean error between the emissions estimates and the ground truth over the entire grid. While `NaiveSearch` and `AdaSearch` have comparable performance over time, we observe that `InfoMax` reduces total Euclidean error quickly at first but is eventually overtaken by both `AdaSearch` and `NaiveSearch`. This is again surprising, since we expect `InfoMax` to excel at total-grid mapping.

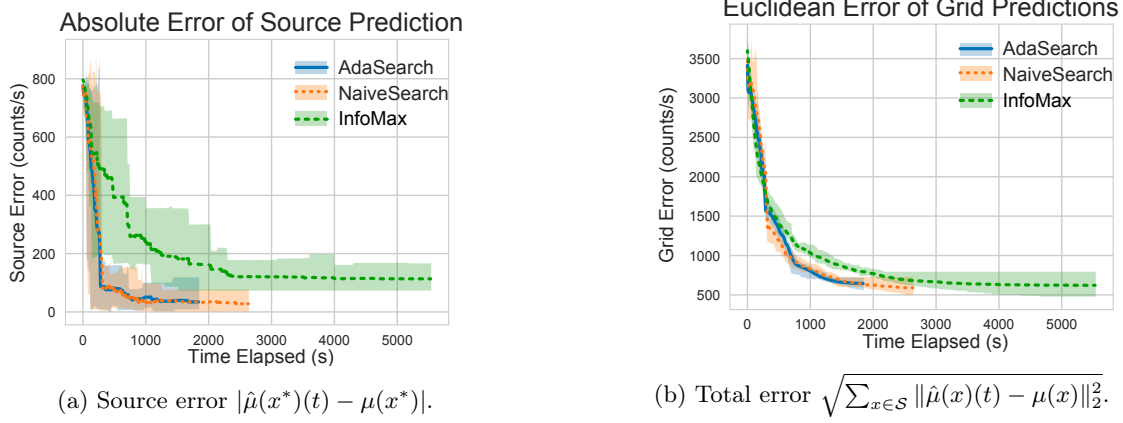


Figure 4: Simulation results of **AdaSearch**, **NaiveSearch** and **InfoMax** based on 10 randomized instantiations with $\bar{\mu} = 400$ and $\mu^* = 800 \frac{\text{counts}}{\text{s}}$. Lighter shaded areas denote the range of values at each time over 10 runs of each algorithm; dark lines show the mean. We include final errors for runs that have already finished in max, min, and mean computations.

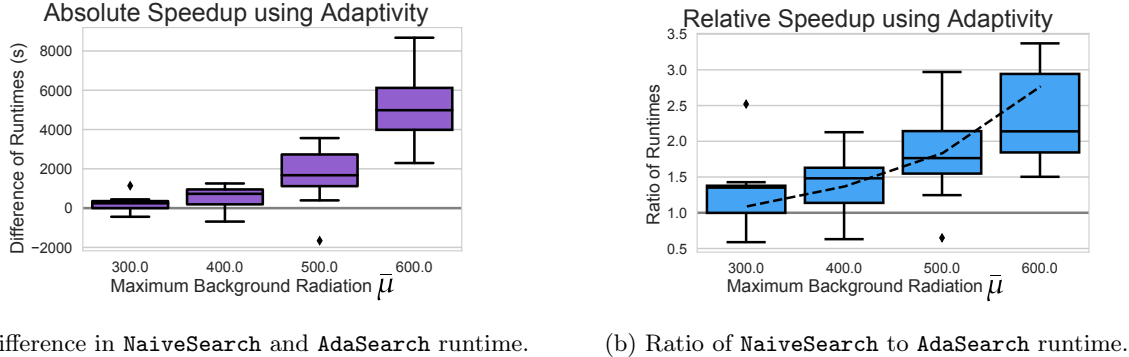


Figure 5: Relative performance of **AdaSearch** and **NaiveSearch** for $\bar{\mu} \in \{300, 400, 500, 600\}$ and $\mu^* = 800 \frac{\text{counts}}{\text{s}}$. Each algorithm was given the same 10 randomized grid instantiations. Box plots show quartile values.

Figure 5b compares relative performance of **NaiveSearch** and **AdaSearch** over the 10 trials. **AdaSearch** consistently outperforms **NaiveSearch**, and the relative speedup increases as $\bar{\mu}$ approaches μ^* . This result is consistent with the theoretical analysis in Sec. 5; the dashed line in Fig. 5b plots a fit curve with rule $0.7 \cdot \mu^*/(\mu^* - \bar{\mu})$ (see discussion below).

Discussion. While all three methods eventually locate the correct source x^* , the two algorithms with global planning heuristics, **AdaSearch** and **NaiveSearch**, terminate considerably earlier than **InfoMax**, which uses a greedy, receding horizon approach (Fig. 3). Moreover, the adaptive algorithm **AdaSearch** consistently terminates before its non-adaptive counterpart, **NaiveSearch**.

As $\bar{\mu}$ approaches μ^* and the gaps $\mu^* - \mu(x)$ become more variable, adaptivity confers even greater advantages over uniform sampling (Fig. 5). Consider the following computation. As shown in Appendix B.3, when $\mu(x) \sim \text{Unif}(0, \bar{\mu})$, the sample complexities for **AdaSearch** and **NaiveSearch** in (17) simplify to $\tilde{\mathcal{O}}(|\mathcal{S}|(\mu^* - \bar{\mu})^{-1})$ and $\tilde{\mathcal{O}}(|\mathcal{S}|\mu^*(\mu^* - \bar{\mu})^{-2})$, respectively. Hence, we expect the ratio of **NaiveSearch** runtime to **AdaSearch** runtime to scale as $\mu^*/(\mu^* - \bar{\mu})$, which is corroborated by the fit of the dashed line to average relative performance in Fig. 5b.

The **AdaSearch** algorithm excels when it can quickly rule out points in early rounds. From (17) we recall that the **AdaSearch** sample complexity scales with the average value of $\mu(x)/(\mu^* - \mu(x))^2$ (rather than the maximum, for **NaiveSearch**). Hence, **AdaSearch** will outperform **NaiveSearch** when there are varying levels

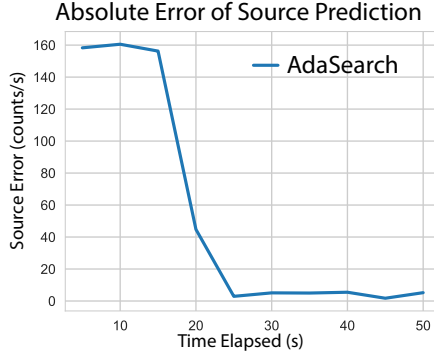


Figure 6: Hardware demonstration of **AdaSearch**. Difference between the estimated emission rate at the true source and the true emission rate $|\hat{\mu}_{x^*}(t) - \mu_{x^*}|$, recorded over time during a representative run.

of background radiation and some points have emission rates close to μ^* (see Fig. 5b). However, the doubling procedure in **AdaSearch** may be wasteful, and result in over-measuring on the last round. This may occur when all background points have emission rates considerably lower than μ^* (see $\bar{\mu} = 300$ in Fig. 5).

InfoMax’s strength lies in quickly reducing global uncertainty across the entire emissions landscape. However, **InfoMax** takes considerably longer to identify x^* (Fig. 3) and, surprisingly, **AdaSearch** and **NaiveSearch** ultimately outperform **InfoMax** in mapping the entire emissions landscape on longer time scales (Fig. 4b). We attribute this to the effects of greedy, receding horizon planning. Initially, **InfoMax** has many locally-promising points to explore and reduces the Euclidean error quickly. Later on, it becomes harder to find informative trajectories that route the quadrotor near the few under-explored regions. This suggests that when a path \mathcal{Z} such as the raster path used here is available, it is well worth considering.

Hardware results. The previous results are based on a simulation of two key physical processes: radiation sensing and vehicle dynamics. The Poisson model of radioactive emissions and sensing is common in the literature [30]; however, there are varying degrees of accuracy in modeling vehicle dynamics. In order to validate the results of our simulation study in the presence of the inevitable mismatch between the near-hover dynamics model and true quadrotor dynamics, we test **AdaSearch** on a Crazyflie 2.0 palm-sized quadrotor in a motion capture room (Fig. 1). The motion capture data (position and orientation) is acquired at roughly 235 Hz and processed in real-time using precisely the same implementation of **AdaSearch** as was used in our software simulations. Our supplementary video shows a more detailed display of our system.² Fig. 1 shows a visualization of the confidence intervals, and the absolute source point estimation error, during a representative flight over a small 4×4 grid, roughly 3 m on a side. After two rounds, **AdaSearch** has identified the two highest emitting points as the highlighted pixels in the inset in Fig. 1. At this point, the absolute error in estimating $\mu(x^*)$ is very small (see Fig. 6). For the remainder of the flight, **AdaSearch** spends most of its time sensing these two points and avoids taking too many redundant measurements elsewhere in the grid. The general pattern of performance matches the simulation results in Fig. 4a (solid blue).

7 Generalizations and Extensions

Unknown number of sources. If the number of sources is initially unknown, then running **AdaSearch** with small k will result in measurements that are still informative about all true sources, since they must be distinguished from the top k sources. This could result in sufficient measurement coverage, or it could inform the choice of a larger k .

Oriented sensor. A natural extension of our radioactive source-seeking example is to consider a sensing model with a sensitivity function that depends upon orientation. Here, the additional challenge lies in identifying informative sensing configuration sets \mathcal{Z}_i , and a reasonably efficient equivalent fixed global path \mathcal{Z} . More broadly, the sensing configurations $z \in \mathcal{Z}$ could be taken to represent generalized configurations of the robot and sensor, e.g. they could encode the position and angular orientation of a directional sensor, or

²A video summarizing this work is available at: https://people.eecs.berkeley.edu/~erolf/adasearch_5mins.m4v.

joint angles of a manipulator arm.

Pointwise sensing model. We motivated the pointwise sensing model where sensitivity function is $h(x, z) = \mathbb{I}\{x = z\}$ as a model conducive to theoretical analysis. Though it is only a coarse (yet still predictive) approximation of the physical process of radiation sensing, this sensitivity model is a more precise descriptor of other adaptive sensing processes, for example, survey design. As a concrete example, suppose an aid group with enough funding to set up k medical clinics sought to identify which k towns had the highest rates of disease. It is reasonable to think that the data collected about village i is mostly informative about only the rate of disease in that town, so that the pointwise sensing model may be quite appropriate.

Surveying. Although we demonstrate **AdaSearch** operating onboard a UAV in the context of RSS, the core algorithm applies more broadly, even to non-robotic embodied sensing problems. Consider the problem of planning k clinic locations introduced about. Because surveys are conducted in person, the aid group is resource limited in terms of using human surveyors, both in terms of the time it takes to survey a single person or clinic within a town, and in terms of travel time between towns. A survey planner could use **AdaSearch** to guide the decisions of how long to spend in each town counting new cases of the disease before moving on to the next, and to trade-off the travel time of returning to collect more data from a certain town with spending extra time at the town in the first place.

While **AdaSearch** provides a good starting point for solving such problems, the high cost of transportation would likely make it worthwhile to further optimize the surveying trajectory at each round, e.g. by (approximately) solving a traveling salesman problem.

8 Conclusion

In summary, we have demonstrated that statistical methods from pure exploration active learning offer a promising and under-explored toolkit for adaptive sensing. Specifically, we have shown that motion constraints need not impede active learning strategies, and highlighted incorporating realistic measurement models as fertile ground for future research.

Our main contribution, **AdaSearch**, outperforms a greedy information-maximization baseline. Its success can be understood as a consequence of two structural phenomena: planning horizon and implicit design objective. The information-maximization baseline operates on a receding horizon and seeks to reduce global uncertainty, which means that even if its planned trajectories are individually highly informative, they may lead to suboptimal performance over a long time scale. In contrast, **AdaSearch** uses an application-dependent global path that provides efficient coverage of the entire search space, and allocates measurements using principled, statistical confidence intervals.

AdaSearch excels in situations with a heterogeneous distribution of the signal of interest; it would be interesting to make a direct comparison with GP-based methods in a domain where the smooth GP priors are more appropriate. We also plan to explore active sensing in more complex environments and with dynamic signal sources and more sophisticated sensors (e.g. directional sensors). Furthermore, as **AdaSearch** is explicitly designed for general embodied sensing problems, it would be exciting to test it in a wider variety of application domains.

Acknowledgments

This material is based upon work supported by the National Science Foundation Graduate Research Fellowship under Grant No. DGE 1752814.

References

- [1] Kai Vetter, Ross Barnowski, Andrew Haefner, Tenzing HY Joshi, Ryan Pavlovsky, and Brian J. Quiter. Gamma-Ray Imaging for Nuclear Security and Safety: Towards 3-D Gamma-Ray Vision. *Nuclear Instruments and Methods in Physics Research Section A: Accelerators, Spectrometers, Detectors and Associated Equipment*, 878:159–168, 2018.
- [2] Frank Mascarich, Taylor Wilson, Christos Papachristos, and Kostas Alexis. Radiation Source Localization in GPS-denied Environments using Aerial Robots. In *ICRA*. IEEE, 2018.
- [3] Gabriel M Hoffmann and Claire J Tomlin. Mobile sensor network control using mutual information methods and particle filters. *IEEE Trans. on Auto. Control*, 55(1):32–47, 2010.
- [4] Chetan D Pahlajani, Jianxin Sun, Ioannis Poulakakis, and Herbert G Tanner. Error probability bounds for nuclear detection: Improving accuracy through controlled mobility. *Automatica*, 50(10):2470–2481, 2014.
- [5] Roman Marchant and Fabio Ramos. Bayesian Optimisation for Informative Continuous Path Planning. In *ICRA*, pages 6136–6143. IEEE, 2014.
- [6] Matthew Dunbabin and Lino Marques. Robots for environmental monitoring: Significant advancements and applications. *IEEE Robotics & Auto. Mag.*, 19(1):24–39, 2012.
- [7] Frederic Bourgault, Alexei A Makarenko, Stefan B Williams, Ben Grocholsky, and Hugh F Durrant-Whyte. Information based adaptive robotic exploration. In *IROS*, volume 1, pages 540–545. IEEE, 2002.
- [8] Lauren M Miller, Yonatan Silverman, Malcolm A MacIver, and Todd D Murphey. Ergodic exploration of distributed information. *IEEE Trans. on Robotics*, 32(1):36–52, 2016.
- [9] Shi Bai, Jinkun Wang, Fanfei Chen, and Brendan Englot. Information-Theoretic Exploration with Bayesian Optimization. In *IROS*, pages 1816–1822. IEEE, 2016.
- [10] Yifei Ma, Roman Garnett, and Jeff G Schneider. Active Search for Sparse Signals with Region Sensing. In *AAAI*, pages 2315–2321, 2017.
- [11] Benjamin Charrow, Sikang Liu, Vijay Kumar, and Nathan Michael. Information-Theoretic Mapping using cauchy-schwarz quadratic mutual information. In *ICRA*, pages 4791–4798. IEEE, 2015.
- [12] Roman Marchant and Fabio Ramos. Bayesian Optimisation for Intelligent Environmental Monitoring. In *IROS*, pages 2242–2249. IEEE, 2012.
- [13] Ruben Martinez-Cantin, Nando de Freitas, Eric Brochu, José Castellanos, and Arnaud Doucet. A Bayesian Exploration-Exploitation Approach for Optimal Online Sensing and Planning with a Visually Guided Mobile Robot. *Autonomous Robots*, 27(2):93–103, 2009.
- [14] Carlos Guestrin, Andreas Krause, and Ajit Paul Singh. Near-optimal sensor placements in gaussian processes. In *ICML*, pages 265–272. ACM, 2005.
- [15] Nikolay Atanasov, Jerome Le Ny, Kostas Daniilidis, and George J Pappas. Information Acquisition with Sensing Robots: Algorithms and Error Bounds. In *ICRA*, pages 6447–6454. IEEE, 2014.
- [16] Gregory Hitz, Alkis Gotovos, Marie-Éve Garneau, Cédric Pradalier, Andreas Krause, Roland Y Siegwart, et al. Fully autonomous focused exploration for robotic environmental monitoring. In *ICRA*, pages 2658–2664. IEEE, 2014.
- [17] Eyal Even-Dar, Shie Mannor, and Yishay Mansour. Action Elimination and Stopping Conditions for the Multi-Armed Bandit and Reinforcement Learning Problems. *JMLR*, 7(Jun):1079–1105, 2006.
- [18] Jean-Yves Audibert and Sébastien Bubeck. Best Arm Identification in Multi-Armed Bandits. In *COLT*, pages 13–p, 2010.

- [19] Kevin Jamieson, Matthew Malloy, Robert Nowak, and Sébastien Bubeck. lil'UCB: An Optimal Exploration Algorithm for Multi-Armed Bandits. In *COLT*, pages 423–439, 2014.
- [20] Tomer Koren, Roi Livni, and Yishay Mansour. Multi-Armed Bandits with Metric Movement Costs. In *NIPS*, pages 4122–4131, 2017.
- [21] Sébastien Bubeck, Michael B. Cohen, James R. Lee, Yin Tat Lee, and Aleksander Madry. k-server via multiscale entropic regularization. *CoRR*, abs/1711.01085, 2017.
- [22] Niranjan Srinivas, Andreas Krause, Sham M. Kakade, and Matthias W. Seeger. Information-Theoretic Regret bounds for Gaussian Process Optimization in the Bandit Setting. *IEEE Trans. on Info. Theory*, 58(5):3250–3265, 2012.
- [23] Shivaram Kalyanakrishnan, Ambuj Tewari, Peter Auer, and Peter Stone. Pac subset selection in stochastic multi-armed bandits. 2012.
- [24] Emrah Bıyık and Murat Arcak. Gradient Climbing in Formation via Extremum Seeking and Passivity-based Coordination Rules. *Asian Journal of Control*, 10(2):201–211, 2008.
- [25] Alexey S Matveev, Michael C Hoy, and Andrey V Savkin. Extremum Seeking Navigation without Derivative Estimation of a Mobile Robot in a Dynamic Environmental Field. *IEEE Trans. on Control Sys. Tech.*, 24(3):1084–1091, 2016.
- [26] Boaz Porat and Arye Nehorai. Localizing Vapor-Emitting Sources by Noving Sensors. *IEEE Trans. on Sig. Proc.*, 44(4):1018–1021, 1996.
- [27] Luma K. Vasiljevic and Hassan K. Khalil. Error Bounds in Differentiation of Noisy Signals by High-Gain Observers. *Systems & Control Letters*, 57(10):856–862, 2008.
- [28] Ruben Martinez-Cantin. BayesOpt: A Bayesian Optimization Library for Nonlinear Optimization, Experimental Design and Bandits. *JMLR*, 15:3915–3919, 2014.
- [29] Morgan Quigley, Ken Conley, Brian P. Gerkey, Josh Faust, Tully Foote, Jeremy Leibs, Rob Wheeler, and Andrew Y. Ng. ROS: an Open-Source Robot Operating System. In *ICRA Workshop on Open Source Software*, 2009.
- [30] Kenneth Lange, Richard Carson, et al. EM Reconstruction Algorithms for Emission and Transmission Tomography. *J Comput Assist Tomogr*, 8(2):306–316, 1984.
- [31] Max Simchowitz, Kevin Jamieson, and Benjamin Recht. Best-of-K Bandits. In *COLT*, pages 1440–1489, 2016.
- [32] Stéphane Boucheron, Gábor Lugosi, and Pascal Massart. *Concentration Inequalities: A Nonasymptotic Theory of Independence*. Oxford university press, 2013.
- [33] Emilie Kaufmann, Olivier Cappé, and Aurélien Garivier. On the Complexity of Best-Arm Identification in Multi-Armed Bandit Models. *JMLR*, 17(1):1–42, 2016.

Appendix

A Proof of Lemma 1

We verify Lemma 1 given in Section 3. The proof of this lemma holds *for any* instantiation of Algorithm 1, regardless of the sensing model or the planning strategy.

First, we verify that for each round $i \geq 0$, $\mathcal{S}_i^{\text{top}} \cap \mathcal{S}_i = \emptyset$. Indeed, at round $i = 0$, $\mathcal{S}_0^{\text{top}} = \emptyset$, so the bound holds immediately. Suppose by an inductive hypothesis that $\mathcal{S}_i^{\text{top}} \cap \mathcal{S}_i = \emptyset$ for some $i \geq 0$. Then, for any $x \in \mathcal{S}_{i+1}^{\text{top}}$, we have two cases:

- (a) $x \in \mathcal{S}_i^{\text{top}}$. Then, $x \notin \mathcal{S}_i$ by the inductive hypothesis, and $\mathcal{S}_i \supset \mathcal{S}_{i+1}$ by (5).
- (b) x is added to $\mathcal{S}_{i+1}^{\text{top}}$ via (4). Then $x \notin \mathcal{S}_{i+1}$ by (5).

Next, we verify that if the confidence intervals are correct in all rounds leading up to round i , i.e.

$$\text{for all rounds } j \leq i \text{ and all } x \in \mathcal{S}_j, \quad \mu(x) \in (\text{LCB}_j(x), \text{UCB}_j(x)), \quad (13)$$

then $\mathcal{S}_{i+1}^{\text{top}} \subset \mathcal{S}^*(k)$, and $\mathcal{S}^*(k) \subset \mathcal{S}_{i+1}^{\text{top}} \cup \mathcal{S}_{i+1}$. We again use induction. Initially, we have $\mathcal{S}_0^{\text{top}} = \emptyset \subset \mathcal{S}^*(k) \subset \mathcal{S} = \mathcal{S}_0$. Now, suppose that at round i , one has that $\mathcal{S}_i^{\text{top}} \subset \mathcal{S}^*(k)$, and $\mathcal{S}^*(k) \subset \mathcal{S}_i^{\text{top}} \cup \mathcal{S}_i$.

To show that $\mathcal{S}_{i+1}^{\text{top}} \subset \mathcal{S}^*(k)$, it suffices to show that if x is added to $\mathcal{S}_{i+1}^{\text{top}}$, then $x \in \mathcal{S}^*(k)$. By the inductive hypothesis there exists $k - |\mathcal{S}_i^{\text{top}}|$ elements of $\mathcal{S}^*(k)$ in \mathcal{S}_i . Hence, if x is added to $\mathcal{S}_{i+1}^{\text{top}}$, and if (13) holds, then

$$\begin{aligned} \mu(x) &\geq \text{LCB}_i(x) \\ &> (k - |\mathcal{S}_i^{\text{top}}| + 1)\text{-th largest value of UCB}_i(x), \quad x \in \mathcal{S}_i && \text{by (4)} \\ &\geq (k - |\mathcal{S}_i^{\text{top}}| + 1)\text{-th largest value of } \mu(x), \quad x \in \mathcal{S}_i && \text{by (13)} \\ &\geq (k + 1)\text{-th largest value of } \mu(x), \quad x \in \mathcal{S}_i \cup \mathcal{S}_i^{\text{top}}. \end{aligned}$$

Hence, $\mu(x)$ is among the k largest values of $\mu(x)$ for $x \in \mathcal{S}_i \cup \mathcal{S}_i^{\text{top}}$. Since $\mathcal{S}^*(k) \subset \mathcal{S}_i \cup \mathcal{S}_i^{\text{top}}$, we therefore have that $x \in \mathcal{S}^*(k)$.

Similarly, to show $\mathcal{S}^*(k) \subset \mathcal{S}_{i+1} \cup \mathcal{S}_{i+1}^{\text{top}}$, it suffices to show that if $x \in \mathcal{S}_i \setminus \mathcal{S}_{i+1}$, and $x \notin \mathcal{S}_{i+1}^{\text{top}}$, then $x \notin \mathcal{S}^*(k)$. For x such that $x \in \mathcal{S}_i \setminus \mathcal{S}_{i+1}$, and $x \notin \mathcal{S}_{i+1}^{\text{top}}$, it follows that

$$\begin{aligned} \mu(x) &\leq \text{UCB}_i(x) \\ &< (k - |\mathcal{S}_{i+1}^{\text{top}}|)\text{-th largest value of LCB}_i(x), \quad x \in \mathcal{S}_i && \text{by (5)} \\ &\leq (k - |\mathcal{S}_{i+1}^{\text{top}}|)\text{-th largest value of } \mu(x), \quad x \in \mathcal{S}_i && \text{by (13)} \\ &\leq k\text{-th largest value of } \mu(x), \quad x \in \mathcal{S}_i \cup \mathcal{S}_{i+1}^{\text{top}} \\ &\leq k\text{-th largest value of } \mu(x), \quad x \in \mathcal{S}, \end{aligned}$$

hence $\mu(x) \notin \mathcal{S}^*(k)$.

Finally, we verify that if (13) holds at each round, then at the termination round i_{fin} , $\mathcal{S}_{i_{\text{fin}}} = \emptyset$, so that $\mathcal{S}_{i_{\text{fin}}}^{\text{top}} \subset \mathcal{S}^*(k) \subset \mathcal{S}_{i_{\text{fin}}}^{\text{top}} \cup \mathcal{S}_{i_{\text{fin}}} = \mathcal{S}_{i_{\text{fin}}}^{\text{top}}$, so that $\mathcal{S}^*(k) = \mathcal{S}_{i_{\text{fin}}}^{\text{top}}$.

B Theoretical Results for Pointwise Sensing

In this appendix, we present formal statements of the measurement complexities provided in Sec. 5 in the main text, and generalize them to the full top- k problem presented in Algorithm 1 of the main text. We also provide specialized bounds for the randomly generated grids considered in our simulations.

Notation: Throughout, we shall use the notation $f \lesssim g$ to denote that there exists a universal constant C , independent of problem parameters, for which $f \leq C \cdot g$. We also define $\log_+(x) := \max\{1, \log x\}$.

Formal Setup. Throughout, we consider a rectangular grid \mathcal{S} of $|\mathcal{S}|$ points, and let $\mu(x)$ denote the mean emission rate of each point $x \in \mathcal{S}$ in counts/second. We let $\mu^{(k)}$ denote the k -th largest mean $\mu(x)$. In the case that $k = 1$, we denote $\mu^* := \mu^{(1)}$, and let $x^* := \arg \max_{x \in \mathcal{S}} \mu(x)$ denote the highest-mean point, with emission rate $\mu^* := \mu(x^*)$. For identifiability, we assume $\mu^{(k)} > \mu^{(k+1)}$.

Measurements. As described in the main text, we assume a point-wise sensing model in which **AdaSearch** and **NaiveSearch** can measure each point directly. Recall that, at each round i , **AdaSearch** takes $\tau_i := 2^i \tau_0$ measurements at each point $x \in \mathcal{S}_i$, and **NaiveSearch** takes τ_i measurements at each $x \in \mathcal{S}$. We let $\mathbf{N}_i(x)$ denote the total number of counts collected at position x at round i . We further assume that $\mu(x)$ are standardized according to the same time units as τ_0 , measuring a source of mean $\mu(x)$ for time interval of length τ_i yields counts distributed according to $\mathbf{N}_i \sim \text{Poisson}(2^i \cdot \mu(x))$. Finally, we shall let i_{fin} denote the (random) round at which a given algorithm - either **AdaSearch** or **NaiveSearch** - terminates.

Confidence Intervals At the core of our analysis are rigorous $1 - \delta$ upper and lower confidence intervals for Poisson random variables, proved in Sec. E.1:

Proposition 3 *Fix any $\mu \geq 0$ and let $\mathbf{N} \sim \text{Poisson}(\mu)$. Define*

$$U_+(\mathbf{N}, \delta) := 2 \log(1/\delta) + \mathbf{N} + \sqrt{2\mathbf{N} \log(1/\delta)} \quad \text{and} \quad U_-(\mathbf{N}, \delta) := \max \left\{ 0, \mathbf{N} - \sqrt{2\mathbf{N} \log(1/\delta)} \right\} \quad (14)$$

Then, it holds that $\Pr[\mu > U_+(\mathbf{N}, \delta)] \leq \delta$ and $\Pr[\mu < U_-(\mathbf{N}, \delta)] \leq \delta$.

At each round i and $x \in \mathcal{S}_i$ (**AdaSearch**) or $x \in \mathcal{S}$ (**NaiveSearch**), recall that we use upper and lower confidence intervals

$$\text{LCB}_i(x) := \frac{1}{\tau_i} U_-(\mathbf{N}_i(x), \delta_i) , \quad \text{UCB}_i(x) := \frac{1}{\tau_i} U_+(\mathbf{N}_i(x), \delta_i) , \quad \text{where } \delta_i := \delta / (4|\mathcal{S}|i^2).$$

Trajectory for AdaSearch. **AdaSearch** follows a trajectory where, at each round i , **AdaSearch** spends time $\tau_i = 2^i \cdot \tau_0$ measuring each $x \in \mathcal{S}_i$, and spends τ_0 travel time traveling over each $x \notin \mathcal{S}_i$. For the radioactive sensing problem, this is achieved by following the “snaking pattern” depicted in Fig. 2a in the main text, in which the quadrotor speeds up or slows down over each point to match the specified measurement times. We will define the *total sample complexity* and *total run time* respectively as

$$T^{\text{sample}} := \sum_{i=0}^{i_{\text{fin}}} \tau_i |\mathcal{S}_i| \quad \text{and} \quad T^{\text{run}} := T^{\text{sample}} + \sum_{i=0}^{i_{\text{fin}}} \tau_0 |\mathcal{S} \setminus \mathcal{S}_i|$$

The first quantity above captures the total number of measurements taken at points we still wish to measure, and the second captures the total flight time of the algorithm. For simplicity, we will normalize our units of time so that $\tau_0 = 1$.

Trajectory for NaiveSearch. Whereas we implement **NaiveSearch** to travel at a constant speed at each point for each round, our analysis will consider a variant where **NaiveSearch** halves its speed each round - that is, takes 2^i measurements at each point for each round; this doubling yields slightly better bounds on sample complexity, and makes **NaiveSearch** compare even more favorably compared to **AdaSearch** in theory.³ This results in a total of $2^i \tau_0 |\mathcal{S}|$ measurements per round. For **NaiveSearch**, the total sample complexity and total run time are equal, and given by

$$T^{\text{run}} = T^{\text{sample}} = |\mathcal{S}| \sum_{i=0}^{i_{\text{fin}}} \tau_i.$$

Termination Criterion for NaiveSearch: For an arbitrary number of k emitters, **NaiveSearch** terminates at the first round i in which the k -th largest lower confidence bound of all points $x \in \mathcal{S}$ is higher than the $(k+1)$ -th largest upper confidence bound of all points $x \in \mathcal{S}$.

³In practice, we keep the speed constant between trials because, for uniform sampling, this is more efficient; that is, in both theory and practical evaluations, we choose the variant of **NaiveSearch** performs the best

B.1 Main Results for $k = 1$ Emitters

We are now ready to state our main theorems for $k = 1$ emitters. Recall the divergence terms

$$d(\mu_1, \mu_2) := \frac{(\mu_2 - \mu_1)^2}{\mu_2}, \quad (\mu_1 < \mu_2) \quad (15)$$

and, in particular,

$$d(\mu(x), \mu^*) := \frac{(\mu^* - \mu(x))^2}{\mu^*}, \quad (\mu(x) < \mu^*)$$

from Section 5. When term $d(\mu(x), \mu^*)$ is small, it is difficult to distinguish between x^* and x . The following lemma shows that $d(\mu(x), \mu^*)$ approximates the the KL-divergence between the distribution $\text{Poisson}(\mu(x))$ and $\text{Poisson}(\mu^*)$:

Lemma 4 *There exists universal constants c_1 and c_2 such that, for any $\mu_2 \geq \mu_1 > 0$,*

$$c_1 \cdot d(\mu_1, \mu_2) \leq \text{KL}(\text{Poisson}(\mu_1), \text{Poisson}(\mu_2)) \leq c_2 \cdot d(\mu_1, \mu_2), \quad (16)$$

where $d(\mu_1, \mu_2) = (\mu_2 - \mu_1)^2 / \mu_2$.

Up to log factors, the sample complexities for **AdaSearch** and **NaiveSearch** in the $k = 1$ case are given by $\mathcal{C}_{\text{adapt}}$ and $\mathcal{C}_{\text{unif}}$, respectively, as defined in Proposition 2 of the main text and restated below:

$$\mathcal{C}_{\text{adapt}} := \sum_{x \in \mathcal{S} \setminus \{x^*\}} \left(\tau_0 + \frac{1}{d(\mu(x), \mu^*)} \right) \quad \text{and} \quad \mathcal{C}_{\text{unif}} = |\mathcal{S}| \left(\tau_0 + \max_{x \in \mathcal{S}} \frac{1}{d(\mu(x), \mu^*)} \right), \quad (17)$$

$\mathcal{C}_{\text{adapt}}$ and $\mathcal{C}_{\text{unif}}$ differ in that $\mathcal{C}_{\text{adapt}}$ considers the sum over all these point-wise complexities, whereas $\mathcal{C}_{\text{unif}}$ replaces this sum with the number of points multiplied by the worst per-point complexity. $\mathcal{C}_{\text{adapt}}$ can be thought of as the complexity of sampling each point $x \neq x^*$ the exact number of times to distinguish it from x^* , whereas $\mathcal{C}_{\text{unif}}$ is the complexity of sampling each point the exact number of times to distinguish the best point from *every other* point. Note that we always have that $\mathcal{C}_{\text{adapt}} \leq \mathcal{C}_{\text{unif}}$, and in fact $\mathcal{C}_{\text{unif}}$ can be as large as $\mathcal{C}_{\text{adapt}} \cdot |\mathcal{S}|$.

Our first theorem bounds the *sample complexity* of **AdaSearch** for the $k = 1$ case presented in Sec. 5 in the main text. We recall that the sample complexity is the total time spent at all $x \in \mathcal{S}_i$ until termination:

Theorem 5 *For any $\delta \in (0, 1)$, the following holds with probability at least $1 - \delta$: **AdaSearch** correctly returns x^* , the total sample complexity is bounded by bounded above by*

$$T^{\text{sample}} \lesssim |\mathcal{S}| + \sum_{x \neq x^*} \frac{\log_+ \left(|\mathcal{S}| \log_+ \left(\frac{1}{d(\mu(x), \mu^*)} \right) / \delta \right)}{d(\mu(x), \mu^*)} = \tilde{\mathcal{O}} \left(|\mathcal{S}| + \sum_{x \neq x^*} \frac{\log(|\mathcal{S}|/\delta)}{d(\mu(x), \mu^*)} \right),$$

and the runtime is bounded above by

$$T^{\text{run}} \lesssim T^{\text{sample}} + |\mathcal{S}| \log_+ \left(\log_+ \frac{|\mathcal{S}|}{\delta} \cdot \max_{x \neq x^*} \frac{1}{d(\mu(x), \mu^*)} \right) = \tilde{\mathcal{O}} \left(\mathcal{C}_{\text{adapt}} \log(|\mathcal{S}|/\delta) + \tau_0 |\mathcal{S}| \log \left(\frac{\mathcal{C}_{\text{unif}}}{|\mathcal{S}|} \right) \right),$$

where $\tilde{\mathcal{O}}(\cdot)$ hides the doubly logarithmic factors in $1/d(\mu(x), \mu^*)$.

Theorem 5 is a direct consequence of our more general bound for $k \geq 1$ emitters, given by Theorem 8, which is proved in Sec. C. The next proposition, proved in Sec. D, controls the sample complexity of **NaiveSearch**:

Theorem 6 *For any $\delta \in (0, 1)$, the following holds with probability at least $1 - \delta$: **NaiveSearch** correctly returns x^* , and the total runtime is bounded by bounded above by*

$$T^{\text{run}} \lesssim |\mathcal{S}| \cdot \left(\max_{x \neq x^*} \frac{\log_+ \left(|\mathcal{S}| \log_+ \left(\frac{1}{d(\mu(x), \mu^*)} \right) / \delta \right)}{d(\mu(x), \mu^*)} \right) = \tilde{\mathcal{O}}(\mathcal{C}_{\text{unif}} \log(|\mathcal{S}|/\delta)).$$

Lastly, we show that our adaptive and uniform sample complexities are near optimal. We prove the following proposition lower bounding the number of samples any adaptive algorithm must take, in Sec. F.1:

Proposition 7 *There exists a universal constant c such that, for any $\delta \in (0, 1/4)$, any adaptive sampling which correctly identifies the top emitting point x^* with probability at least $1 - \delta$ must collect at least*

$$c \log(1/\delta) \cdot \mathcal{C}_{\text{adapt}}$$

samples in expectation. Moreover, any uniform sampling allocation which identifies the top emitting point x^ with probability at least $1 - \delta$ must take at least*

$$c \log(1/\delta) \cdot \mathcal{C}_{\text{unif}}$$

samples in expectation.

B.2 Analysis for Top- k Poisson Emitters

In this section, we continue our analysis of `AdaSearch`, addressing the full problem of identifying the k Poisson emitters with the highest emission rates. Our goal is to identify the unique set

$$\mathcal{S}^*(k) := \{x \in \mathcal{S} : \mu(x) \geq \mu^{(k)}\} \quad (18)$$

To ensure the top- k emitters are unique, we assume that $\mu^{(k)} > \mu^{(k+1)}$ (recall that $\mu^{(k)}$ denotes the k -th largest value of $\mu(x)$ among all $x \in \mathcal{S}$). The complexity of identifying the top- k emitters can then be described in terms of the gaps of the divergence terms

$$\begin{aligned} d(\mu^{(k+1)}, \mu(x)) &= \frac{(\mu(x) - \mu^{(k+1)})^2}{\mu(x)}, \quad (\mu(x) > \mu^{(k+1)}) \quad \text{and} \\ d(\mu(x), \mu^{(k)}) &= \frac{(\mu^{(k)} - \mu(x))^2}{\mu^{(k)}}, \quad (\mu(x) < \mu^{(k)}). \end{aligned}$$

For $x \in \mathcal{S}^*(k)$, $d(\mu^{(k+1)}, \mu(x))$ describes how close the emission rate $\mu(x)$ is to the “best” alternative in $\mathcal{S} \setminus \mathcal{S}^*(k)$. For $x \in \mathcal{S} \setminus \mathcal{S}^*(k)$, $d(\mu(x), \mu^{(k)})$ describes how close $\mu(x)$ is to the mean $\mu^{(k)}$ of the emitter in $\mathcal{S}^*(k)$ from which it is hardest to distinguish. The analogues of $\mathcal{C}_{\text{adapt}}$ and $\mathcal{C}_{\text{unif}}$ are then

$$\mathcal{C}_{\text{adapt}}^{(k)} := \sum_{x \in \mathcal{S}^*(k)} \frac{1}{d(\mu^{(k+1)}, \mu(x))} + \sum_{x \in \mathcal{S} \setminus \mathcal{S}^*(k)} \frac{1}{d(\mu(x), \mu^{(k)})} \quad \text{and} \quad (19)$$

$$\mathcal{C}_{\text{unif}}^{(k)} := |\mathcal{S}| \cdot \max \left\{ \max_{x \in \mathcal{S}^*(k)} \frac{1}{d(\mu^{(k+1)}, \mu(x))}, \max_{x \in \mathcal{S} \setminus \mathcal{S}^*(k)} \frac{1}{d(\mu(x), \mu^{(k)})} \right\} = |\mathcal{S}| d(\mu^{(k+1)}, \mu^{(k)}) \quad (20)$$

where the equality follows by noting that the function $(x, a) \mapsto \frac{x}{(x-a)^2}$ is decreasing in x and increasing in a for $x > a$. The following theorem, proved in Sec. C, provides an upper bound on the sample complexity for top- k identification:

Theorem 8 *For any $\delta \in (0, 1)$, the following holds with probability at least $1 - \delta$: `NaiveSearch` correctly returns $\mathcal{S}^*(k)$, and the total sample complexity is bounded above by*

$$\begin{aligned} T^{\text{sample}} &\lesssim |\mathcal{S}| + \sum_{x \in \mathcal{S}^*(k)} \frac{\log_+ \left(|\mathcal{S}| \log_+ \left(\frac{1}{d(\mu^{(k+1)}, \mu(x))} \right) \right) / \delta}{d(\mu^{(k+1)}, \mu(x))} + \sum_{x \in \mathcal{S} \setminus \mathcal{S}^*(k)} \frac{\mu^{(k)} \log_+ \left(|\mathcal{S}| \log_+ \left(\frac{1}{d(\mu(x), \mu^{(k)})} \right) \right) / \delta}{d(\mu(x), \mu^{(k)})} \\ &= \tilde{\mathcal{O}} \left(\mathcal{C}_{\text{adapt}}^{(k)} \cdot \log(|\mathcal{S}|/\delta) \right), \end{aligned}$$

and the total runtime is bounded by

$$T^{\text{run}} \lesssim T^{\text{sample}} + |\mathcal{S}| \log_+ \left(\frac{\log_+ \frac{|\mathcal{S}|}{\delta}}{d(\mu^{(k+1)}, \mu^{(k)})} \right) = \tilde{\mathcal{O}} \left(\mathcal{C}_{\text{adapt}}^{(k)} \cdot \log \frac{|\mathcal{S}|}{\delta} + |\mathcal{S}| \log_+ \left(\frac{\mathcal{C}_{\text{unif}}^{(k)}}{|\mathcal{S}|} \right) \right)$$

We remark that our sample complexity qualitatively matches standard bounds for active top- k identification with sub-Gaussian rewards in the non-embodied setting (see, e.g. [23]). Our results differ by considering the appropriate modifications for Poisson emissions, as well as accounting for total travel time. Lastly, we have the bound for uniform sampling.

Theorem 9 *For any $\delta \in (0, 1)$, the following holds with probability at least $1 - \delta$: `NaiveSearch` correctly returns $\mathcal{S}^*(k)$, and the total runtime is bounded by bounded above by*

$$T^{\text{run}} \lesssim \tilde{\mathcal{O}}(\mathcal{C}_{\text{unif}}) \cdot \log(|\mathcal{S}|/\delta).$$

B.3 Predictions for Simulations

We now return to the case $k = 1$. We justify the estimates of the complexity terms $\mathcal{C}_{\text{adapt}}$ and $\mathcal{C}_{\text{unif}}$ provided in Sec. 5 of the main text, where $\mu(x) \sim \text{Unif}[0, \bar{\mu}]$ for $x \neq x^*$, and $|\mathcal{S}| = 256$. To control the complexity of `NaiveSearch`, we observe that

$$\mathcal{C}_{\text{unif}} = \tilde{\mathcal{O}}\left(\max_{x \neq x^*} \frac{1}{d(\mu(x), \mu^*)}\right) = \tilde{\mathcal{O}}\left(\frac{\mu^*}{(\mu^* - \max_{x \neq x^*} \mu(x))^2}\right).$$

It is well known that the maximum of N uniform random variables on $[0, 1]$ is approximately $1 - \Theta(\frac{1}{N})$ with probability $1 - \Theta(\frac{1}{N})$, which implies that $\max_{x \neq x^*} \mu(x) \approx (1 - \frac{1}{|\mathcal{S}|})\bar{\mu} \approx \bar{\mu}$ with probability at least $1 - \Theta(\frac{1}{|\mathcal{S}|})$. Hence, the sample complexity of `NaiveSearch` should scale as

$$\tilde{\mathcal{O}}\left(\frac{|\mathcal{S}|\mu_*}{(\bar{\mu} - \mu_*)^2}\right)$$

On the other hand, the sample complexity of `AdaSearch` grows as

$$\tilde{\mathcal{O}}\left(\sum_{x \neq x^*} \frac{1}{d(\mu(x), \mu^*)}\right) = \tilde{\mathcal{O}}\left(\sum_{x \neq x^*} \mu^*(\mu^* - \mu(x))^{-2}\right)$$

When $\mu(x) \sim \text{Unif}[0, \bar{\mu}]$ are random and $|\mathcal{S}|$ is large, the law of large numbers implies that this term tends to $\tilde{\mathcal{O}}(\mu^*|\mathcal{S}| \cdot \mathbb{E}_{\mu(x) \sim \text{Unif}[0, \bar{\mu}]} (\mu^* - \mu(x))^{-2})$. We can then compute

$$\begin{aligned} \mathbb{E}_{\mu(x) \sim \text{Unif}[0, \bar{\mu}]} (\mu^* - \mu(x))^{-2} &= \frac{1}{\bar{\mu}} \int_0^{\bar{\mu}} \frac{1}{(\mu^* - t)^2} dt = \frac{1}{\bar{\mu}} \int_{\mu^* - \bar{\mu}}^{\mu^*} \frac{1}{u^2} du \\ &= \frac{1}{\bar{\mu}} \frac{1}{\mu^* - \bar{\mu}} - \frac{1}{\mu^*} = \frac{1}{\bar{\mu}} \frac{\mu^* - (\mu^* - \bar{\mu})}{(\mu^* - \bar{\mu})\mu^*} \\ &= \frac{1}{\bar{\mu}} \frac{\bar{\mu}}{(\mu^* - \bar{\mu})\mu^*} = \frac{1}{(\mu^* - \bar{\mu})\mu^*}, \end{aligned}$$

Hence, the total complexity scales as

$$\tilde{\mathcal{O}}(\mu^*|\mathcal{S}| \cdot \mathbb{E}_{\mu(x) \sim \text{Unif}[0, \bar{\mu}]} (\mu^* - \mu(x))^{-2}) = \tilde{\mathcal{O}}(|\mathcal{S}|(\mu^* - \bar{\mu})^{-1})$$

Therefore, the ratio of the runtimes of `AdaSearch` to `NaiveSearch` are

$$\frac{\mu^* - \bar{\mu}}{\mu^*} = 1 - \frac{\bar{\mu}}{\mu^*}.$$

C Analyzing AdaSearch: Proof of Theorem 8

C.1 Analysis Roadmap

To simplify the analysis, we assume that at round i , we take a fresh $\tau_i = 2^i$ samples (recall we have normalized $\tau_0 = 1$) from each remaining $x \in \mathcal{S}_i$.⁴ For $x \in \mathcal{S}_i$, $\mathbf{N}_i(x)$ denotes the number of counts observed from point x

⁴The analysis is nearly the same as if we used the total $2^{i+1} - 1$ samples collected throughout.

over the interval of length τ_i , and $\widehat{\mu}_i(x)$ denotes the empirical average emissions; that is, $\widehat{\mu}_i(x) = \mathbf{N}_i(x)/\tau_i$. With this notation, our confidence intervals take the following form:

$$\text{LCB}_i(x) := \frac{1}{2^i} U_- \left(\mathbf{N}_i(x), \frac{\delta}{4|\mathcal{S}|i^2} \right) \text{ and } \text{UCB}_i(x) := \frac{1}{2^i} U_+ \left(\mathbf{N}_i(x), \frac{\delta}{4|\mathcal{S}|i^2} \right) \quad (21)$$

We first argue that there exists a good event, $\mathcal{E}_{\text{good}}(\delta)$, occurring with probability at least $1 - \delta$, on which the true mean $\mu(x)$ of each pixel x lies between $\text{LCB}_i(x)$ and $\text{UCB}_i(x)$ for all i . Moreover, $\text{LCB}_i(x)$ and $\text{UCB}_i(x)$ are contained within the interval defined by $[\overline{\text{UCB}}_i(x), \overline{\text{LCB}}_i(x)]$, which depends explicitly upon $\mu(x)$, but *not* on $\widehat{\mu}_i(x)$. To derive $\overline{\text{UCB}}_i(x)$ and $\overline{\text{LCB}}_i(x)$, we begin by deriving high probability upper and lower bounds $\overline{U}_+(\mu, \delta)$ and $\overline{U}_-(\mu, \delta)$ for the functions $U_+(\mathbf{N}, \delta)$ and $U_-(\mathbf{N}, \delta)$ that hold for Poisson random variables. Formally, we have the following

Proposition 10 *Let $\mu \geq 0$ and let $\mathbf{N} \sim \text{Poisson}(\mu)$. Define*

$$\begin{aligned} \overline{U}_+(\mu, \delta) &:= \mu + \frac{14}{3} \log(1/\delta) + 2\sqrt{2\mu \log(1/\delta)} \quad \text{and} \\ \overline{U}_-(\mu, \delta) &:= \max \left\{ 0, \mu - 2\sqrt{2\mu \log(1/\delta)} \right\}. \end{aligned}$$

Then, it holds that

$$\Pr [\overline{U}_-(\mu, \delta) \leq U_-(\mathbf{N}, \delta) \leq \mu \leq U_+(\mathbf{N}, \delta) \leq \overline{U}_+(\mu, \delta)] \geq 1 - 2\delta. \quad (22)$$

As a consequence of Proposition 10, we can show that $\overline{\text{LCB}}_i(x)$ and $\overline{\text{UCB}}_i(x)$ are probabilistic lower and upper bounds on $\text{LCB}_i(x)$ and $\text{UCB}_i(x)$:

Lemma 11 *Introduce the confidence intervals*

$$\overline{\text{LCB}}_i(x) := \frac{1}{\tau_i} \overline{U}_- \left(\tau_i \mu(x), \frac{\delta}{4|\mathcal{S}|i^2} \right) \text{ and } \overline{\text{UCB}}_i(x) := \frac{|\mathcal{S}|}{\tau_i} \overline{U}_+ \left(\tau_i \mu(x), \frac{\delta}{4|\mathcal{S}|i^2} \right).$$

Then, there exists an event $\mathcal{E}_{\text{good}}$ for which $\Pr[\mathcal{E}_{\text{good}}] \geq 1 - \delta$, and

$$\forall i \geq 1, x \in \mathcal{S}_i : \overline{\text{LCB}}_i(x) \leq \text{LCB}_i(x) \leq \mu(x) \leq \text{UCB}_i(x) \leq \overline{\text{UCB}}_i(x). \quad (23)$$

Lemma 11 is a simple consequence of Propositions 3 and 10, and a union bound; it is proved formally in Sec C.3. Note that on $\mathcal{E}_{\text{good}}$, one has that $\mu(x) \in [\text{LCB}_i(x), \text{UCB}_i(x)]$ for all rounds i and all $x \in \mathcal{S}_i$; hence, by Lemma 1,

Lemma 12 *If $\mathcal{E}_{\text{good}}$ holds, then for all rounds i , $\mathcal{S}_i^{\text{top}} \subset \mathcal{S}^*(k) \subset \mathcal{S}_i^{\text{top}} \cup \mathcal{S}_i$; in particular, if **AdaSearch** terminates at round i_{fin} , then it correctly returns $\mathcal{S}^*(k)$.*

Finally, the next lemma, proven in C.4, gives a *deterministic* condition under which a point $x \in \mathcal{S}$ can be removed from \mathcal{S}_i , in terms of the deterministic confidence bounds $\overline{\text{LCB}}_i(x)$ and $\overline{\text{UCB}}_i(x)$.

Lemma 13 *Suppose $\mathcal{E}_{\text{good}}$ holds. Let $x^{(k)}$ and $x^{(k+1)}$ denote arbitrary points in \mathcal{S} with $\mu(x^{(k)}) = \mu^{(k)}$ and $\mu(x^{(k)}) = \mu^{(k)}$. Define the function*

$$i_{\text{fin}}(x) := \begin{cases} \inf \{i : \overline{\text{LCB}}_i(x) > \overline{\text{UCB}}_i(x^{(k+1)})\} & x \in \mathcal{S}^*(k) \\ \inf \{i : \overline{\text{UCB}}_i(x) < \overline{\text{LCB}}_i(x^{(k)})\} & x \in \mathcal{S} \setminus \mathcal{S}^*(k) \end{cases}$$

Then, on $\mathcal{E}_{\text{good}}$, $x \notin \mathcal{S}_i$ for all $i > i_{\text{fin}}(x)$.

In view of Lemma 13, we can bound

$$\begin{aligned} T^{\text{sample}} &:= \sum_{i=0}^{i_{\text{fin}}} \tau_i |\mathcal{S}_i| = \sum_{x \in \mathcal{S}} \sum_{i \geq 0} \tau_i \mathbb{I}(x \in \mathcal{S}_i) \leq \sum_{x \in \mathcal{S}} \sum_{i=0}^{i_{\text{fin}}(x)} \tau_i \quad (\text{by Lemma 13}) \\ &\leq \sum_{x \in \mathcal{S}} 2^{i_{\text{fin}}(x)+1} \quad (\text{since } \tau_i = 2^i) \end{aligned} \quad (24)$$

and further, bound

$$\begin{aligned} T^{\text{run}} &:= T^{\text{sample}} + \sum_{i=0}^{i_{\text{fin}}} \tau_0 |\mathcal{S} \setminus \mathcal{S}_i| \leq T^{\text{sample}} + |\mathcal{S}| i_{\text{fin}} \quad (\text{recall } \tau_0 = 1) \\ &\leq T^{\text{sample}} + |\mathcal{S}| \max_{x \in \mathcal{S}} i_{\text{fin}}(x). \end{aligned} \quad (25)$$

where again the last line uses Lemma 13. Lastly, we prove an upper bound on $i_{\text{fin}}(x)$ for all $x \in \mathcal{S}$, which follows from algebraic manipulations detailed in Sec. C.2:

Proposition 14 *There exists a universal constant $C > 1$ such that, for $x \in \mathcal{S}^*(k)$,*

$$2^{i_{\text{fin}}(x)} \leq C \cdot \left\{ 1 + \frac{\log_+ \left(|\mathcal{S}| \log_+ \left(\frac{1}{d(\mu^{(k+1)}, \mu(x))} \right) / \delta \right)}{d(\mu^{(k+1)}, \mu(x))} \right\}$$

whereas for $x \in \mathcal{S} \setminus \mathcal{S}^*(k)$,

$$2^{i_{\text{fin}}(x)} \leq C \cdot \left\{ 1 + \frac{\log_+ \left(|\mathcal{S}| \log_+ \left(\frac{1}{d(\mu^{(k+1)}, \mu(x))} \right) / \delta \right)}{d(\mu^{(k+1)}, \mu(x))} \right\}$$

Theorem 8 now follows by plugging in Proposition 14 into Equations (24) and (25).

C.2 Proof of Proposition 14

Let $n = 2^i$, let $\delta_0 = \delta / (4|\mathcal{S}| \log_2 e)$, and let $\Delta = \mu(x_1) - \mu(x_2)$. Then $\overline{\text{UCB}}_i(x_2) < \overline{\text{LCB}}_i(x_1)$ is equivalent to $\mu(x_2) + \frac{14}{3n} \log(\delta_0^{-1} \log n) + 2\sqrt{2\mu(x_2) \log(\delta_0^{-1} \log n) / n} < \mu(x_1) - 2\sqrt{2\mu(x_1) \log(\delta_0^{-1} \log n) / n}$ implied by $\frac{14}{3n} \log(\delta_0^{-1} \log n) + 4\sqrt{2\mu(x_1) \log(\delta_0^{-1} \log n) / n} < \Delta$,

where the second line uses $\mu(x_2) \leq \mu(x_1)$. For the second line to hold, it is enough that

$$\frac{1}{n} \log(\delta_0^{-1} \log n) < \frac{3\Delta}{28} \text{ and } \log(\delta_0^{-1} \log n) / n < \left(\frac{\Delta}{8\sqrt{2}} \right)^2 \quad (26)$$

We now invoke an inversion lemma from the best arm identification literature (see, e.g. Equation (110) in [31]).

Lemma 15 *For any $\delta, u > 0$, let $\mathcal{T}(u, \delta) := 1 + \log_+(\delta^{-1} \log_+(u)) / u$. There exists a universal constant C_0 such that, for all $n \geq C_0 \mathcal{T}(u, \delta)$, we have $\log(\delta^{-1} \log n) / n < u$.*

Hence, Lemma 15 and (26) imply that it is sufficient that

$$n \geq C_0 \mathcal{T} \left(\min \left\{ \frac{3\Delta}{28}, \frac{1}{\mu(x_1)} \left(\frac{\Delta}{8\sqrt{2}} \right)^2 \right\}, \delta_0 \right),$$

from which it follows that

$$\inf \{2^i : \overline{\text{UCB}}_i(x_2) < \overline{\text{LCB}}_i(x_1)\} \leq 2C_0 \left\{ \mathcal{T} \left(\min \left\{ \frac{3\Delta}{28}, \frac{1}{\mu(x_1)} \left(\frac{\Delta}{8\sqrt{2}} \right)^2 \right\}, \delta_0 \right) \right\}$$

Absorbing constants and plugging in $\delta_0 = \delta / (4|\mathcal{S}| \log_2 e)$, algebraic manipulation finally implies that there exists a universal constant C such that, for any x_1, x_2 with $\mu(x_1) < \mu(x_2)$,

$$\begin{aligned} \inf \{2^i : \overline{\text{UCB}}_i(x_1) < \overline{\text{LCB}}_i(x_2)\} &\leq C \left\{ 1 + \mathcal{T} \left(\min \left\{ \Delta, \frac{\Delta^2}{\mu(x_1)} \right\}, \delta/M \right) \right\} \\ &= C \left\{ 1 + \mathcal{T} \left(\frac{\Delta^2}{\mu(x_1)}, \delta/|\mathcal{S}| \right) \right\} \\ &= C \{1 + \mathcal{T}(d(\mu(x_2), \mu(x_1)), \delta/|\mathcal{S}|)\}. \end{aligned}$$

To conclude, we select $x_1 = x^{(k+1)}$ and $x_2 = x$ when $x \in \mathcal{S}^*(k)$, and $x_1 = x$ and $x_2 = x^{(k)}$ for $x \in \mathcal{S} \setminus \mathcal{S}^*(k)$.

C.3 Proof of Lemma 11

$$\begin{aligned}
& \Pr \left[\exists x \in \mathcal{S}_0, i \geq 1 : \{\overline{\text{LCB}}_i(x) \leq \text{LCB}_i(x) \leq \mu(x) \leq \text{UCB}_i(x) \leq \overline{\text{UCB}}_i(x)\} \text{ fails} \right] \\
& \stackrel{\text{union bound}}{\leq} \sum_{x \in \mathcal{S}_0, i \geq 1} \Pr \left[\{\overline{\text{LCB}}_i(x) \leq \text{LCB}_i(x) \leq \mu(x) \leq \text{UCB}_i(x) \leq \overline{\text{UCB}}_i(x)\} \text{ fails} \right] \\
& \stackrel{\text{Prop. 3\&10}}{\leq} \sum_{x \in \mathcal{S}_0, i \geq 1} \frac{\delta}{2|\mathcal{S}|i^2} = |\mathcal{S}| \sum_{i \geq 1} \frac{\delta}{2|\mathcal{S}|i^2} = \frac{\delta}{2} \sum_i i^{-2} \leq \delta.
\end{aligned}$$

C.4 Proof of Lemma 13

Assume $\mathcal{E}_{\text{good}}$ holds, and let $x \in \mathcal{S}$, and set $i = i_{\text{fin}}(x)$. Then

- (a) If $x \in \mathcal{S}^*(k)$, then $\overline{\text{LCB}}_i(x) > \overline{\text{UCB}}_i(x^{(k+1)})$. In this case, we shall show that x will be added to $\mathcal{S}_i^{\text{top}}$ via (4).
- (b) If $x \in \mathcal{S} \setminus \mathcal{S}^*(k)$, then $\overline{\text{UCB}}_i(x) < \overline{\text{LCB}}_i(x^{(k)})$. In this case, we shall show that x will be removed from \mathcal{S}_i via (5).

Case 1: $\overline{\text{LCB}}_i(x) > \overline{\text{UCB}}_i(x^{(k+1)})$ By (4), x is added to $\mathcal{S}_{i+1}^{\text{top}}$ if $\text{LCB}_i(x)$ is larger than all but $k - |\mathcal{S}_i^{\text{top}}|$ values of $\text{UCB}_i(x')$, $x' \in \mathcal{S}_i$. Since $\text{LCB}_i(x) \geq \overline{\text{LCB}}_i(x)$ and $\text{UCB}_i(x') \leq \overline{\text{UCB}}_i(x')$ on $\mathcal{E}_{\text{good}}$, it is enough that

$$\overline{\text{LCB}}_i(x) > (k - |\mathcal{S}_i^{\text{top}}| + 1)\text{-st largest value of } \overline{\text{UCB}}_i(x'), x' \in \mathcal{S}_i.$$

We now observe that $\overline{\text{UCB}}_i(x')$ is monotonic in $\mu(x')$. Hence, it is enough that

$$\overline{\text{LCB}}_i(x) > \overline{\text{UCB}}_i(x_+), \text{ where } \mu(x_+) = (k - |\mathcal{S}_i^{\text{top}}| + 1)\text{-st largest value of } \mu(x'), x' \in \mathcal{S}_i.$$

But since there are exactly $k - |\mathcal{S}_i^{\text{top}}|$ elements of $\mathcal{S}^*(k)$ in \mathcal{S}_i by Lemma 12, x_+ is not among the top k , and thus $\mu(x_+) \leq \mu(x^{(k+1)})$. Hence, $\overline{\text{UCB}}_i(x_+) \leq \overline{\text{UCB}}_i(\mu(x^{(k+1)}))$, so it is enough that $\overline{\text{LCB}}_i(x) > \overline{\text{UCB}}_i(\mu(x^{(k+1)}))$.

Case 2: $\overline{\text{UCB}}_i(x) < \overline{\text{LCB}}_i(x^{(k)})$ Following the reasoning of case 1 applied to (5), we can see that it is enough that

$$\overline{\text{UCB}}_i(x) < \overline{\text{LCB}}_i(x_-), \text{ where } \mu(x_-) = (k - |\mathcal{S}_{i+1}^{\text{top}}|)\text{-st largest value of } \mu(x), x' \in \mathcal{S}_i \setminus \mathcal{S}_{i+1}^{\text{top}}.$$

Lemma 12 ensures that there are $(k - |\mathcal{S}_{i+1}^{\text{top}}|)$ members of $\mathcal{S}^*(k)$ in $\mathcal{S}_i \setminus \mathcal{S}_{i+1}^{\text{top}}$, so $\mu(x_-) \geq \mu(x^{(k)})$. Hence, it is enough that $\overline{\text{UCB}}_i(x) < \overline{\text{LCB}}_i(x^{(k)})$.

D Analysis of NaiveSearch: Proof of Theorem 6

In this section, we present a brief proof of Theorems 6 and 9. The arguments are quite similar to those in the analysis of AdaSearch, and we shall point out modifications as we go along.

Let $\mathcal{E}_{\text{good}}$ denote the event of Lemma 11, modified to hold for all $x \in \mathcal{S}$ at each round i (rather than all $x \in \mathcal{S}_i$, as in the case of AdaSearch). The proof of Lemma 11 extends to this case as well, yielding that

$$\Pr[\mathcal{E}_{\text{good}}] \geq 1 - \delta$$

It suffices to show that on $\mathcal{E}_{\text{good}}$, NaiveSearch correctly returns $\mathcal{S}^*(k)$, and satisfies the desired runtime guarantees.

Correctness: On $\mathcal{E}_{\text{good}}$, we have that $x \in \mathcal{S}^*(k)$, $\mu(x) \leq \text{UCB}_i(x)$, and for $x' \in \mathcal{S} - \mathcal{S}^*(k)$, $\mu(x') \geq \text{LCB}_i(x')$. Hence, for any $x' \in \mathcal{S} - \mathcal{S}^*(k)$ and for all $x \in \mathcal{S}^*(k)$, $\text{LCB}_i(x') \leq \mu(x') < \mu(x) \leq \text{UCB}_i(x')$. Thus, the termination criterion can only be fulfilled when $\text{LCB}_i(x)$, each $x \in \mathcal{S}^*(k)$, are greater than the remained $|\mathcal{S}| - k$ values of $\text{UCB}_i(x)$. This yields correctness.

Runtime: Recall that for `NaiveSearch` with the standardization τ_0 , we have

$$T^{\text{run}} = |\mathcal{S}| \sum_{i=0}^{i_{\text{fin}}} \tau_i = |\mathcal{S}| \sum_{i=0}^{i_{\text{fin}}} 2^i \leq 2|\mathcal{S}| \cdot 2^{i_{\text{fin}}}$$

Arguing as in the analysis for `AdaSearch`, it suffices to show that, on $\mathcal{E}_{\text{good}}$,

$$i_{\text{fin}} \leq \inf\{i : \overline{\text{LCB}}_i(x) > \overline{\text{UCB}}_i(x') \quad \forall x \in \mathcal{S}^*(k), x' \in \mathcal{S} - \mathcal{S}^*(k)\} := \overline{i_{\text{fin}}}, \quad (27)$$

for we bound the the bound

$$\begin{aligned} T^{\text{run}} &\lesssim |\mathcal{S}| 2^{\overline{i_{\text{fin}}}} \\ &\stackrel{(i)}{\lesssim} |\mathcal{S}| \cdot \max_{x \in \mathcal{S}^*(k), x' \in \mathcal{S} - \mathcal{S}^*(k)} \frac{\log_+ \left(\frac{|\mathcal{S}|}{\delta} \log_+ \left(\frac{1}{d(\mu(x'), \mu(x))} \right) \right)}{d(\mu(x'), \mu(x))} \\ &= |\mathcal{S}| \cdot \frac{\log_+ \left(\frac{|\mathcal{S}|}{\delta} \log_+ \left(\frac{1}{d(\mu^{(k+1)}, \mu^{(k)})} \right) \right)}{d(\mu^{(k+1)}, \mu^{(k)})} \\ &= \tilde{O}(\mathcal{C}_{\text{unif}} \log(|\mathcal{S}|/\delta)), \end{aligned}$$

where (i) follows from the same argument as in the proof of Proposition 14. To verify (27), suppose that $\mathcal{E}_{\text{good}}$ holds, and that `NaiveSearch` has not terminated before round $\overline{i_{\text{fin}}}$. Then, by definition of $\overline{i_{\text{fin}}}$,

$$\overline{\text{LCB}}_i(x) > \overline{\text{UCB}}_i(x'), \quad \forall x \in \mathcal{S}^*(k), x' \in \mathcal{S} - \mathcal{S}^*(k)$$

Moreover, on $\mathcal{E}_{\text{good}}$, $\text{LCB}_i(x) \geq \overline{\text{LCB}}_i(x)$ and $\text{UCB}_i(x') \leq \overline{\text{UCB}}_i(x')$ for all $x \in \mathcal{S}^*(k)$ and all $x' \in \mathcal{S} - \mathcal{S}^*(k)$. Thus,

$$\text{LCB}_i(x) > \text{UCB}_i(x'), \quad \forall x \in \mathcal{S}^*(k), x' \in \mathcal{S} - \mathcal{S}^*(k),$$

which directly implies the termination criterion for `NaiveSearch`.

E Concentration Proofs

It is well known that the upper Poisson tail satisfies Bennet's inequality, and its lower tail is sub-Gaussian, yielding the following exponential tail bounds (see, e.g. [32]):

Lemma 16 *Let $\mathbf{N} \sim \text{Poisson}(\mu)$. Then,*

$$\Pr[\mathbf{N} \geq \mu + x] \leq \exp \left(-\frac{x^2}{2(\mu + x/3)} \right) \quad \text{and} \quad \Pr[\mathbf{N} \leq \mu - x] \leq \exp \left(-\frac{x^2}{2\mu} \right) \quad (28)$$

E.1 Proof of Proposition 3

Proof that $\Pr[\mu \leq U_+(\mathbf{N}, \delta)] \geq 1 - \delta$: Recall the definition

$$U_+(\mathbf{N}, \delta) := 2 \log(1/\delta) + \mathbf{N} + \sqrt{2\mathbf{N} \log(1/\delta)}.$$

We begin by bounding the lower tail of \mathbf{N} , which corresponds to the upper confidence U_+ bound on μ . Let $\mathcal{E}_+(\delta)$ denote the event $\{\mathbf{N} \geq \mu - \sqrt{2\mu \log(1/\delta)}\}$. By Lemma 16, we have that $\Pr[\mathcal{E}_+(\delta)^c] \leq \delta$; hence, it suffices to show that

$$\mathcal{E}_+(\delta) \text{ implies } \{\mu \leq U_+(\mathbf{N}, \delta)\}.$$

This follows since by the definition $\mathcal{E}_+(\delta)$ holds, the quadratic equation implies

$$\mu^{1/2} \leq \frac{\sqrt{2 \log(1/\delta)} + \sqrt{2 \log(1/\delta) + 4\mathbf{N}}}{2} \quad (29)$$

Hence, we have

$$\begin{aligned}
\mu &\leq \frac{2\log(1/\delta) + 2\log(1/\delta) + 4\mathbf{N} + 2\sqrt{2\log(1/\delta)}\sqrt{4\mathbf{N} + 2\log(1/\delta)}}{4} \\
&\leq \frac{4\log(1/\delta) + 4\mathbf{N} + 4\log(1/\delta) + 4\sqrt{2\mathbf{N}\log(1/\delta)}}{4} \\
&= 2\log(1/\delta) + \mathbf{N} + \sqrt{2\mathbf{N}\log(1/\delta)} = U_+(\mathbf{N}, \delta) \text{ , as needed.}
\end{aligned}$$

Proof that $\Pr[\mu \geq U_-(\mathbf{N}, \delta)] \geq 1 - \delta$: Recall the definition

$$U_-(\mathbf{N}, \delta) := \max \left\{ 0, \mathbf{N} - \sqrt{2\mathbf{N}\log(1/\delta)} \right\}$$

Analogous to the above, let $\mathcal{E}_-(\delta) := \{\mathbf{N} \leq \mu + \sqrt{2\mu\log(1/\delta)} + \frac{2}{3}\log(1/\delta)\}$. Since $\Pr[\mathbf{N} \geq \mu + x] \leq \exp(-\frac{x^2}{2(\mu+x/3)})$, we have that with probability at least $\Pr[\mathcal{E}_-(\delta)] \geq 1 - \delta$. Thus, again it suffices to show that

$$\mathcal{E}_-(\delta) \text{ implies } \{\mu \geq U_-(\mathbf{N}, \delta)\}.$$

We have two cases:

- (a) $\mathbf{N} \leq \frac{2}{3}\log(1/\delta)$. Then, $U_-(\mathbf{N}, \delta) = 0$, so $\mu \geq U_-(\mathbf{N}, \delta)$ trivially.
- (b) Otherwise, by solving the quadratic in the definition $\mathcal{E}_-(\delta)$, we find that on $\mathcal{E}_-(\delta)$,

$$\begin{aligned}
\mu^{1/2} &\geq \frac{-\sqrt{2\log(1/\delta)} \pm \sqrt{2\log(1/\delta) - \frac{8}{3}\log(1/\delta) + 4\mathbf{N}}}{2} \\
&= \frac{-\sqrt{2\log(1/\delta)} \pm \sqrt{4\mathbf{N} - 2/3\log(1/\delta)}}{2},
\end{aligned}$$

where we note that the discriminant is positive since $\mathbf{N} \geq \frac{2}{3}\log(1/\delta)$. Squaring, we have

$$\begin{aligned}
\mu &\geq \frac{2\log(1/\delta) + 4\mathbf{N} - 2\log(1/\delta)/3 - 2\sqrt{2\log(1/\delta)}\sqrt{4\mathbf{N} - 2/3\log(1/\delta)}}{4} \\
&\geq \frac{4\mathbf{N} + (2 - 2/3)\log(1/\delta) - 4\log(1/\delta)\sqrt{1/3} - 4\sqrt{2\mathbf{N}\log(1/\delta)}}{4} \\
&\geq \mathbf{N} + (1 - 1/6 - \sqrt{1/3})\log(1/\delta) - \sqrt{2\mathbf{N}\log(1/\delta)} \geq \mathbf{N} - \sqrt{2\mathbf{N}\log(1/\delta)}.
\end{aligned}$$

Since we also have $\mu \geq 0$, we see that on $\mathcal{E}_0(\delta)$, we have that

$$\mu \geq \max\{\mathbf{N} - \sqrt{2\mathbf{N}\log(1/\delta)}, 0\} = U_-(\mathbf{N}, \delta), \text{ as needed.}$$

E.2 Proof of Proposition 10

From section E.1, recall the events

$$\mathcal{E}_+(\delta) := \{\mathbf{N} \geq \mu - \sqrt{2\mu\log(1/\delta)}\} \quad \text{and} \quad \mathcal{E}_-(\delta) := \{\mathbf{N} \leq \mu + \sqrt{2\mu\log(1/\delta)} + \frac{2}{3}\log(1/\delta)\}. \quad (30)$$

Further, recall that on $\mathcal{E}_+(\delta)$, we have $\mu \leq U_+(\mathbf{N}, \delta)$ and $\mu \geq U_-(\mathbf{N}, \delta)$. We now show that on $\mathcal{E}_-(\delta)$, we also have $U_+(\mathbf{N}, \delta) \leq \overline{\text{UCB}}(\mu, \delta)$, and on $\mathcal{E}_+(\delta)$, we have $U_-(\mathbf{N}, \delta) \geq \overline{\text{LCB}}(\mu, \delta)$. **Bounding $U_-(\mathbf{N}, \delta) \geq \overline{U}_-(\mu, \delta)$:** To bound $U_-(\mathbf{N}, \delta) \geq \overline{U}_-(\mu, \delta)$, observe that $\mathbf{N} \mapsto U_-(\mathbf{N}, \delta)$ is increasing in \mathbf{N} , and on $\mathcal{E}_+(\delta)$, one has $\{\mathbf{N} \geq \mu - \sqrt{2\mu\log(1/\delta)}\}$. Thus

$$\begin{aligned}
U_-(\mathbf{N}, \delta) &:= \mathbf{N} - \sqrt{2\mathbf{N}\log(1/\delta)} \\
&\geq \mu - \sqrt{2\mu\log(1/\delta)} - \sqrt{2\log(1/\delta)\mu(\mu - \sqrt{2\mu\log(1/\delta)})} \\
&\geq \mu - \sqrt{2\mu\log(1/\delta)} - \sqrt{2\mu\log(1/\delta)} \\
&\geq \mu - 2\sqrt{2\mu\log(1/\delta)} := \overline{U}_-(\mu, \delta).
\end{aligned}$$

Bounding $U_+(\mathbf{N}, \delta) \leq \overline{U}_+(\mu, \delta)$: Next, we prove the bound $U_+(\mathbf{N}, \delta) \leq \overline{U}_+(\mu, \delta)$. On $\mathcal{E}_-(\delta)$, we have

$$\begin{aligned}\mathbf{N} &\leq \mu + \frac{2}{3} \log(1/\delta) + \sqrt{2\mu \log(1/\delta)} \\ &= (\mu^{1/2} + \sqrt{2 \log(1/\delta)})^2 - 2 \log(1/\delta) + \frac{2}{3} \log(1/\delta) \\ &\leq (\mu^{1/2} + \sqrt{2 \log(1/\delta)})^2\end{aligned}$$

Hence, when the above occurs, we have

$$\begin{aligned}U_+(\mathbf{N}, \delta) &= 2 \log(1/\delta) + \mathbf{N} + \sqrt{2\mathbf{N} \log(1/\delta)} \\ &= 2 \log(1/\delta) + \mu + \frac{2}{3} \log(1/\delta) + \sqrt{2\mu \log(1/\delta)} + \sqrt{2((\mu^{1/2} + \sqrt{2 \log(1/\delta)})^2) \log(1/\delta)} \\ &= \frac{8}{3} \log(1/\delta) + \mu + \sqrt{2\mu \log(1/\delta)} + \sqrt{2((\mu^{1/2} + \sqrt{2 \log(1/\delta)})^2) \log(1/\delta)} \\ &\leq \frac{8}{3} \log(1/\delta) + \mu + \sqrt{2\mu \log(1/\delta)} + \sqrt{2\mu \log(1/\delta)} + 2 \log(1/\delta) \\ &= \frac{14}{3} \log(1/\delta) + \mu + 2\sqrt{2\mu \log(1/\delta)}\end{aligned}$$

F Lower Bounds

F.1 Proof of Proposition 7

The basic proof strategy follows along the lines of the information-theoretic lower bounds in Kaufmann et al. '16 [33]. Consider a grid \mathcal{S} of $|\mathcal{S}|$ points, with means $\mu(x), x \in \mathcal{S}$. We fix a given sampling algorithm, adaptive or otherwise, and let $T(x)$ denote the expected number of measurements from point x given that the means are given by $\mu(x)$. Suppose $x^* := \arg \max_{x \in \mathcal{S}} \mu(x)$ is unique. We will argue that for a universal constant c_1 and any $x \neq x^*$,

$$T(x) \geq \frac{c_1 \log(1/\delta)}{\text{KL}(\mu(x), \mu(x^*))}. \quad (31)$$

By the KL approximation in Lemma 4, this implies that for some universal constant c_2 ,

$$T(x) \geq \frac{c_2 \log(1/\delta)}{d(\mu(x), \mu^*)}. \quad (32)$$

For adaptive sampling, the expected number of samples is at least $\sum_{x \neq x^*} T(x)$, which by (32) is at least

$$c_2 \log(1/\delta) \cdot \sum_{x \neq x^*} \frac{\mu(x^*)}{\Delta_x^2}.$$

This completes the proof for adaptive sampling. For non-adaptive sampling, $T(x) = T(x')$ for all $x, x' \in \mathcal{S}$. Hence, the expected number of samples is at least

$$\sum_{x \in \mathcal{S}} T(x) = |\mathcal{S}| \max_{x \neq x^*} T(x) \stackrel{(32)}{\geq} |\mathcal{S}| \cdot \max_{x \neq x^*} c_2 \log(1/\delta) \frac{\mu(x^*)}{\Delta_x^2}.$$

We now verify Equation (31). To do so, consider an alternative grid \mathcal{S}' of $|\mathcal{S}'|$ pixels, with means $\mu'(x)$. Suppose moreover that $x^{*'} := \arg \max_{x \in \mathcal{S}'} \mu'(x)$ is unique, and that $x^* \neq x^{*'}\$. The key insight from Kaufmann et al. '16 [33] is that any algorithm which identifies x^* with probability $1 - \delta$ must be able to distinguish between the means $\mu'(x)$ and the with means $\mu(x)$. Kaufmann et al. '16 [33] shows that this requires that the expected number of samples $T(x)$ satisfy

$$\sum_{x \in \mathcal{S}} T(x) \text{KL}(\mu(x), \mu'(x)) \geq c_1 \log(1/\delta) \quad (33)$$

Now let's fix a particular $x_0 \neq x^*$ and an $\epsilon > 0$. We can define the means $\mu'(x)$ to be

$$\mu'(x) := \begin{cases} \mu(x^*) + \epsilon & x = x_0 \\ \mu(x) & \text{otherwise} \end{cases}$$

Note then that $\arg \max_x \mu'(x) = x_0$, and $\mu(x_0) = \mu(x^*) + \epsilon$. Hence, Equation (33) holds for the means $\mu'(\cdot)$. Moreover, $\mu(x) = \mu'(x)$ for all $x \neq x_0$, so that $\text{KL}(\mu(x), \mu'(x)) = 0$ for $x \neq x_0$. Hence, Equation (33) simplifies to

$$T(x_0) \text{KL}(\mu'(x_0), \mu'(x^*) + \epsilon) = T(x_0) \text{KL}(\mu(x_0), \mu'(x_0)) \geq c_1 \log(1/\delta)$$

Since $\text{KL}(\mu'(x_0), \mu'(x^*) + \epsilon)$ is continuous in ϵ (see Fact 17 below), taking $\epsilon \rightarrow 0$ yields

$$T(x_0) \text{KL}(\mu'(x_0), \mu'(x^*)) \geq c_1 \log(1/\delta) \text{ as needed.}$$

F.2 Proof of Lemma 4

We begin by stating a standard computation of the KL-divergence between two Poisson distributions.

Fact 17 $\text{KL}(\text{Poisson}(\mu_1), \text{Poisson}(\mu_2)) = \mu_1 \log(\mu_1/\mu_2) + (\mu_2 - \mu_1)$.

To prove Lemma 4, recall that we assume that $\mu_2 \geq \mu_1$. We may therefore reparameterize $\mu \leftarrow \mu_2$, and $\mu_1 \leftarrow (1 - \alpha)\mu_2$ for $\alpha \in (0, 1)$. One then has

$$\text{KL}(\text{Poisson}(\mu_1), \text{Poisson}(\mu_2)) = \mu\{\alpha + (1 - \alpha) \log(1 - \alpha)\}$$

Since $\mu_2 - \mu_1 = \mu(1 - (1 - \alpha)) = \alpha\mu$, it suffices to show that there exists constants c_1 and c_2 such that

$$c_1 \mu \alpha^2 \leq \text{KL}(\text{Poisson}(\mu_1), \text{Poisson}(\mu_2)) \leq c_2 \mu \alpha^2 . \quad (34)$$

To this end, it suffices to show that there exists a universal constant $\alpha_0 > 0$, such for all $\alpha \leq \alpha_0$, one has

$$\text{KL}(\text{Poisson}(\mu_1), \text{Poisson}(\mu_2)) \in \left[\frac{1}{4}, \frac{3}{4} \right] \mu \alpha^2 . \quad (35)$$

Indeed, for any $\alpha \geq \alpha_0$, we have that

$$0 < \mu(\alpha_0 + (1 - \alpha_0) \log(1 - \alpha_0)) \leq \text{KL}(\text{Poisson}(\mu_1), \text{Poisson}(\mu_2)) \leq \mu ,$$

which implies that, for $\alpha \in [\alpha_0, 1]$,

$$\begin{aligned} 0 &< (\alpha^2 \mu) \cdot (\alpha_0 + (1 - \alpha_0) \log(1 - \alpha_0)) \\ &\leq \alpha^2 \mu \cdot \frac{\alpha_0 + (1 - \alpha_0) \log(1 - \alpha_0)}{\alpha^2} \\ &\leq \text{KL}(\text{Poisson}(\mu_1), \text{Poisson}(\mu_2)) \\ &\leq \alpha^2 \mu \cdot \frac{1}{\alpha^2} \leq (\mu \alpha^2) \cdot \frac{1}{\alpha_0^2} . \end{aligned}$$

Hence taking $c_1 = (\alpha_0 + (1 - \alpha_0) \log(1 - \alpha_0))$ and $c_2 = \frac{1}{\alpha_0^2}$, we see that (34) holds for $\alpha \in [\alpha_0, 1]$. We now turn to prove (35). Note that $\log'(1 - x) = -1/(1 - x)$, $\log''(1 - x) = 1/(1 - x)^2$, and $\log'''(x) = -2/(1 - x)^3$. Hence, by Taylor's theorem, there exists an $\alpha' \in [0, \alpha]$ such that

$$\begin{aligned} \log(1 - \alpha) &= \alpha \log'(1) + \frac{\alpha^2}{2} \log''(1) + \frac{\alpha^3}{6} \log'''(1 - \alpha') \\ &= -\alpha - \frac{\alpha^2}{2} - \frac{2\alpha^3}{(1 - \alpha')^3} . \end{aligned}$$

Hence,

$$\begin{aligned}
\text{KL}(\text{Poisson}(\mu_1), \text{Poisson}(\mu_2)) &= \mu \left\{ \alpha - (1-\alpha)(\alpha + \frac{\alpha^2}{2} + \frac{2\alpha^3}{(1-\alpha')^3}) \right\} \\
&= \mu \left\{ \alpha - (1-\alpha)(\alpha + \frac{\alpha^2}{2} + \frac{2\alpha^3}{(1-\alpha')^3}) \right\} \\
&= \mu \left\{ \alpha - \alpha - \frac{\alpha^2}{2} - \frac{2\alpha^3}{(1-\alpha')^3} + \alpha^2 + \frac{\alpha^3}{2} + \frac{2\alpha^4}{(1-\alpha')^3} \right\} \\
&= \mu \left\{ \frac{\alpha^2}{2} + \alpha^3 \left(\frac{-2}{(1-\alpha')^3} + \frac{1}{2} + \frac{2\alpha}{(1-\alpha')^3} \right) \right\} .
\end{aligned}$$

In particular, there exists a universal constant α_0 such that, for all $\alpha \leq \alpha_0$,

$$\text{KL}(\text{Poisson}(\mu_1), \text{Poisson}(\mu_2)) \in \left[\frac{1}{4}, \frac{3}{4} \right] \mu \alpha^2 .$$